FACULTY OF PHYSICS

ADAM MICKIEWICZ UNIVERSITY

NANOBIOMEDICAL CENTER

DEPARTMENT OF MOLECULAR BIOPHYSICS

POZNAŃ 2015

pNiPAM nanoparticles suspensions as model crowded complex systems: synthesis, characterization and properties

Tobiasz Deptuła

Supervisor: Prof. dr hab. Adam Patkowski

Doctoral Thesis

This work was supported by the International PhD Projects Program (”The PhD in Nanoscience and Nanotechnology”) Foundation for polish Science operated within the Innovative Economy Operational Programme (IE OP) 2007-2013 within European Regional Fund.

Oświadczenie autora pracy

Ja niżej podpisany mgr Tobiasz Deptuła oświadczam, ze przedkładaną rozprawę doktorską pt.:

"pNiPAM nanoparticles suspensions as crowded complex model systems: synthesis, characterization and properties."

Napisałem samodzielnie. Oznacza to, ze przy pisaniu pracy, poza niezbędnymi konsultacjami nie korzystałem z pomocy innych osób, a w szczególności nie zlecałem opracowania rozprawy lub jej istotnej części innym osobom, ani nie odpisywałem tej rozprawy lub jej istotnych części od innych osób.

Oświadczam ponadto, ze wydrukowana oraz elektroniczna wersja pracy są identyczne.

Podziękowania:

Panu profesorowi ***Adamowi Patkowskiemu*** ze opiekę promotorską, za życzliwość, wyrozumiałość, poświęcony czas oraz za dzielenie się wiedzą.

Panu profesorowi ***Jackowi Gapińskiemu*** za cenne wskazówki podczas pracy, wsparcie oraz cierpliwość.

Panu profesorowi ***Stefanowi Jurdze*** za przyjęcie do zespołu badawczego oraz umożliwienie mi realizacji pracy doktorskiej.

Dziękuję moim rodzicom i bratu za wsparcie i nieskończoną wiarę we mnie.

Dla Marty...

ABBREVIATION

AIBN - 2,2-azobis(2-methylopropioitrile)

BIS - N,N-methylenebisacrylamide

CF - correlation function

CPM - counts per molecule

Cryo-SEM - Cryogenic Scanning Electron Microscope

DEAAm - N,N-diethylacrylamide

DDS - drug delivery system

DFS – Dynamic Frequency Sweep

DLS - dynamic light scattering

DMEM - Dulbecco's modified Eagle's - Sigma

DMSO - dimethyl sulfoxide

EDTA- Ethylenediaminetetraacetic acid

FBS - fetal bovine serum

FCS fluorescence correlation spectroscopy

FITC - Fluorescein isothiocyanate isomer I

GPC - Gel permeation chromatography

HeK293 - human embryonic kidney cell line

HeLa - cervical cancer cell line

LAOS - Large Amplitude Oscillatory Shear

LCST - lower critical solution temperature

MTT - dimethylthiazol biphenyl tetrazolium bromide

NMR - Nuclear magnetic resonance

NP's - nanoparticles

OD - optical density

PEG - polyethylene glycol

PEO - polyethylene oxide

pNiPAM - poly-N-isopropylarcylamide

PPO - polypropeleneoxide

PVCL - poly-N-vinylcaprolactam

RAFT - Reversible Addition Fragmentation Transfer

SDS - Sodium dodecyl sulfate

SE – Stockes – Einstein

SEM - Scanning Electron Microscope

TA - Particle Tracking Analysis

TCC - Tri-cyclohexyl carbodiimide

TEA - triethylamine

THF - tetrahydrofuran

TABLE OF CONTENT

ABSTRACT

Improvements in controlled polymer synthesis and characterization methods have lead scientists to investigate new materials that would not only improve old techniques, but also open way for new approaches in several industrial and bio-medical applications. Poly-N-isopropylacrylamide (pNiPAM) is one example among this new class of materials. Being respondent to variations in temperature this 'intelligent' polymer is widely considered as a model system that is a promising candidate for biomaterials, drug delivery systems, biosensors, bioanalytical devices or bio-scaffolds for cell cultures. Wide range of potential applications of these nanoparticles arises mostly from their nanometric size and tunable properties. Various types of pNiPAM nanoparticles with its lower critical solution temperature (LCST), around natural human body temperature (at 33^{o}C) were synthesized and characterized in terms of size and morphology. Additionally to study the mechanical properties of pNiPAM microgel, oscillation rheology investigations in the absence and in the presence of linear pNiPAM chains additives were performed. Next step was to establish an efficient way for chemical labeling of the polymeric nanoparticles with a fluorescent dye. Such pNiPAM nanoparticles were suitable for fluorescent techniques which allowed using them as model systems to study diffusion process and micro/macro viscosity effect in crowded complex systems. Additionally a correction procedure to study the size of relatively large, uniformly labeled nanoparticles in FCS experiment was proposed. Finally, conducted cytotoxicity studies, not only proved the lack of toxic effect but additionally demonstrated a pNiPAM bio-scaffold based growth promotion effect on cell cultures.

STRESZCZENIE

Postęp w stosowaniu polimerowych materiałów zarówno w przemyśle jak i w biomedycynie, koncentruje uwagę naukowców na polimerach wykazujących właściwości konkurencyjne w stosunku do tradycyjnych materiałów. Polimery tworzące struktury w skali nano stanowią obiecujące narzędzie o szerokim spektrum zastosowań jako biomateriały, biosensory, systemy dostarczania leków czy bio-podłoża do hodowli komórkowych. Jednym z takich polimerów jest pNiPAM (poly-N-isoporpylacrylamid), który dzięki temperaturze przejścia fazowego (Lower Critical Solution Temperature) około naturalnej temperatury ciała ludzkiego (33^{o}C) zasługuje na szczególną uwagę. Przeprowadzono syntezę różnego rodzaju nanocząstek polimeru pNiPAM oraz szczegółową charakterystykę pod kątem rozmiaru i morfologii otrzymanych struktur. Dodatkowo w celu określenia właściwości mechanicznych przeprowadzono oscylacyjne badania reologiczne samego mikrożelu oraz w obecności liniowych łańcuchów polimeru pNiPAM. Funkcjonalizacja nanocząstek za pomocą chemicznego wprowadzenia wydajnego fluorescencyjnie barwnika w strukturę nanocząstek pNiPAM, umożliwiła ich zastosowanie w technikach fluorescencyjnych. Umożliwiło to użycie nanocząstek pNiPAM jako modelowego systemu do badania dyfuzji w gęstych układach złożonych oraz do badań nad micro/macro lepkością. Zaproponowano także poprawkę do procedury pomiaru wielkości, relatywnie dużych, jednolicie wyznakowanych nanocząstek przy użyciu techniki FCS. Dodatkowo ze względu szeroką gammę zastosowań w biologii i biotechnologii przeprowadzono badania nad cytotoksycznością otrzymanych nanocząstek. Stwierdzono brak efektu cytotoksyczności i ponadto zaobserwowano przyspieszenie wzrostu komórek w obecności nanocząstek pNiPAM. Tym samym zaproponowano nowe potencjalne zastosowanie nanostruktur pNiPAM jako rusztowania do wzrostu komórek.

1. INTRODUCTION

Since centuries people around the globe in many different cultures and civilizations were defined by the materials that they used. Starting with prehistoric periods called Stone Age, Bronze Age and finally Iron Age this three-age system created by Christian Thomsen proves that indeed the adoption of certain materials coincided with other changes in society thus it is reasonable to use it for classifying societies and their stages of progress. Based on this, a question on which materials we, twenty first century people are using seems quite natural and clearly an obvious answer is – polymers. Polymers in fact play crucial role in everyday life; first our body is made out of a lot of polymers like proteins and nucleic acids secondly, naturally occurring polymers are truly serving humans for hundreds of decades e.g. rubber, wood, leather and silk. Moreover we based our industry on fossil fuels (petroleum/oil) and besides we are using it mainly as a fuel, it did revolutionize the processing of the polymers. Introduction of petroleum in the industry have opened new possibilities for exploring and investigating the wide group of materials called synthetic polymers. They emerged simultaneously with oil based industrial revolution and it did not take long for these new materials to spread in everyday usage. As a result the knowledge about natural and synthetic polymers has been developed – which, as mentioned before, were improved in recent years along with the petroleum applications. Can one clearly say that in fact we are living in a polymer age? In recent decades we learn that in fact it is so. Of course some naturally occurring polymers the one that our body is

made of starting with nucleic acids along with proteins and, enzymes and ones that come from human surrounding like wood (cellulose), leather, rubber, and silk are serving the humankind for centuries but improvements in modern tools revolutionized the processing of polymers. Thus, synthetic polymers like plastics, rubbers and fiber materials today are commonly available. The main problem about every single material that we are using is its properties and these properties are strictly related to the constituent structural elements and their arrangement. Since we learn how to process synthetic polymers and how we can adjust their properties we almost displaced previously widely used natural materials (wood, stone, etc.). What is the reason we continue to search for better materials and we are pursuing after more specific properties? An answer to this question is not a goal of this work and most probably is a topic of none of which I have heard of. Despite the remaining question lets define what is a polymer than. Coming from Greek originated '*polys' meaning many* and '*mero'* – which means part, the word polymer means material consisting of many/poly parts/mers. Once the meaning is clear I would like to come back to essence of polymers – which are their unique properties and have a closer look on what is crucial for controlling these properties. Although the fundamental property of synthetic polymers is the degree of polymerization which defines whether the polymer is linear or branched, the physical structure of the single chains is also an important factor that determines the properties. So it seems more accurate to classify polymers according to their mechanical and thermal behavior as plastics (formed or mold

into desire shape) and elastomers (polymers that can undergo different kinds of elongation). Branched polymers based on a cross-linked network among many elastomers can exhibit various properties which will differ greatly depending on a wide range of synthesis procedures with tunable details. In general, the synthesis called polymerization starts from small units (monomers) joined over and over to become a large molecule. The classification based on this is quite complicated but it indicated a crucial factor for designing new materials properties which is polymer architecture including star-branched, H-branched, comb, ladder, dendrimer or randomly branched polymers. Among these structures randomly branched polymers can form polymer networks which can consist of one or more kinds of monomers eventually forming a copolymer structure. As it can be seen any kind of addition of side chains will modify the properties of the polymer product. Within this group of polymers properties can not only be predicted but what is more relevant can be tunable, we call them stimuli – responsive polymers. Since there is a great effort comprising an accelerated convergence of diverse field (such as chemistry, biology, biotechnology, and biophysics) advanced functional materials seem to promise a wide spectrum of applications. In comparison with all living cells which are being regulated by many factors that respond to changes in local environment synthetic polymers with temperature, pH, or even light as the stimulus are considered as a responsive can be called biomimetic and their development leads to emerge application in biology, chemistry physics or medicine.

1.1. Definition of a microgel

Synthetic polymers have gained much of interest in broad range spectrum of fields especially for various medical purposes. New group of nanomedicine which can be used as therapeutic agents, carriers or sensors mostly for anticancer applications have been created. They exhibit an improved pharmacokinetics in comparison to small molecule drugs, meaning longer circulation time, less toxicity and potential tissue targeting. Among many therapeutic and diagnostic applications being used as a drug delivery system emerge clearly as a most promising one. These polymer therapeutics or nanomedicines since all of these materials are within the nanometric size range, can be used as a drug itself forming a polymeric drug or in combination with drugs or molecules resulting in polymeric conjugates with drugs, proteins, nucleic acids or polymeric micelles. Once polymer is not a drug itself it has to fulfil a demand as a safety carrier or agent. This passive function reduces the toxicity and immunogenicity compared to traditional carriers. Also the load is more secured and effective by reducing the degradation and improving its circulation time making it available for a longer period of time for any therapeutic or diagnostic purpose. To fulfil this list of criteria a polymeric carrier has to be water soluble, non-toxic and non-immunogenic and on the top of it all it has to be well design to control it during all stages of drug delivery process. While the toxicity and immunogenicity are considered to be important

the crucial factor for any drug delivery system is a control release of a drug. Therefore a special kind of synthetic polymers deserves more attention – stimuli responsive polymers. They are sensitive to various external factors resulting in a change in properties.

An important group of synthetic polymers are microgels which are cross-linked colloidal polymeric particles with a network structure soluble in suitable solvent like water. According to the definition microgel is simply a particle of gel of any shape with an equivalent diameter of approximately 0.1 to 10 micrometers. It is a non-fluid colloidal network or polymer network that is expanded throughout its whole volume by a fluid/solvent. Due to nano/microscale several advantages such as defined particles structure, loading capacity and targeting potential or even tunable properties triggered by environmental factors have to be pointed out. Additionally, a group of microgels with water as a solvent called hydrogels deserve a closer look. These microgels in which water is being absorbed or retained in the polymeric network, makes hydrogel polymers unique. A typical hydrogel is composed of hydrodrophilic networks that can swell in the presence of a good solvent in particular, meaning water. Three dimension architecture and the unique swelling behavior of a hydrogel are provided by the chemical crosslinks. More specifically, polymeric network enables them to undergo size and volume changes in a response to environmental factors such as changes in pH, temperature, ionic strength [2] [3] [4]. Additionally the electrostatic repulsion or attraction between charged groups in the polymeric network can also results in a

different behavior. This elastic polymer network depending on the incorporated functional groups can be classified as anionic, cationic, neutral or amphiphilic [5]. Based on a size of a cross-linked chain segment colloidal particles with a network structure that are swollen in a suitable solvent microgels can be formed; particle size from 100nm to hundred microns or nanogels in which colloid particles should not be larger than 100nm. As the past decades has shown microgels have been receiving an increasing attention in soft matter studies, both theoretical and applied. Simultaneously, the interest in development of nanoscale materials for numerous industrial or medical applications was growing. Exhibiting environmentally responsive behavior, microgels are being developed for uses in the fields as diverse as nanoscale medicine, bioadhesion devices, biosensors or various kinds of nanoscale technology. Their sensitivity to the thermal environment is clearly the most recognized application for all the responsive polymers with potential applications in the drug delivery systems[6]. This approach has gained importance especially in the last decade since it is a promising tool for pharmaceutical industry. Using nanoparticles in general but also hydrogel nanoparticles as carries for therapeutic drugs or a diagnostic agent becomes a developing technique for everyday use. Creating porous polymeric network hydrogels provides an ideal reservoir for any kind of load such as therapeutic drugs, diagnostic agents or biosensors. The dimension of a particular carrier is an important determinant in loading and realizing kinetics, porosity and drug distribution. Moreover the size of nanoparticles protects the load from

environmental conditions often considered as potential hazards for degradation of a load. Introducing hydrogel polymer carriers has improved the basic properties for every drug which of course is the protection of chemically active substance and moreover the use of the nanoparticles significantly reduces the amount of drug which is necessary to achieve the therapeutic effect. As mentioned before within the hydrogels materials some of them are stimuli responsive and based on this they are called smart or intelligent materials [7]. All living systems respond to external stimuli adapting themselves to changing environment conditions. Synthetic polymers have been trying to mimic this behavior creating the so called smart polymers defined as polymers that undergoes reversible and large, physical or chemical changes in response to relatively small external changes in the environmental conditions, mainly pH and temperature (T). Being responsive to environmental factors is even more interesting in terms of load carrying. The load which at first is incorporated in the porous polymeric network can be released in a response to external factors. Of course this release should be well controlled to take place in a well-defined way and condition. Another aspect of the polymer hydrogels as a carrier is their functionalization. By adding the receptor-specific ligands one can functionalize hydrogels in terms of being cell-specific or even tissue-specific[8]. Combining all of this properties results in achieving very interesting polymer material which properties can be well controlled during the synthesis; consist mostly of water – making it biocompatible; composed of

nanoparticles (reduced size); being responsive to external factors; possible functionalization in terms of targeting the carrier with its load.

1.2. Thermoresponsive poly-N-isopropylacrylamide

Because of its tunable properties and nanometric size most widely investigated for wide spectrum of application the most studied synthetic responsive polymer is poly-N-isopropylarcylamide (pNiPAM). It synthesis was first reported in 1968 and up to date it is a well-known polymer material which exhibits all the 'smart polymer material' features as well controlled synthesis, characterization and possible functionalization of the polymer nanoparticles. Poly-N-isopropylacrylamide (pNiPAM) is one of this new class of materials with wide range of applications as a biomaterials (Drug Delivery Systems) [9,10], biosensors[11] and bioanalytical devices[12] with particle size responding to variations in temperature, pH, ionic strength or hydrostatic pressure [13, 14,15]. Its wide range of application proves that an environmentally responsive material with capability to swell deserves tremendous research interests. Thermoresponsive polymers – pNiPAM in particular have been extensively employed in composite and hybrid materials. Introducing copolymers such as polystyrene or acrylic acid new and unique advantages of pNiPAM can be found. Wide spread application like drug delivery or biosensing are most investigated one but definitely not the latest. PNiPAM nanofibers or hydrogels as scaffold for cell and tissue engineering

application brought a new light for this polymeric hydrogel [16]. Thanks to fact that pNiPAM hydrogel network forms a scaffold on which cells can easily grow and considering its lack of cytotoxicity and numerous potential functionalization possibilities with dyes, nonaparticles or various agents pNiPAM emerges as a one of the most notorious responsive polymers. Recent development of various techniques that are based on grafting a thermoresponsive pNiPAM on the surface of cores based on zinc and iron oxides, gold and silver nanoparticles allowed the birth of smarter systems that can respond to more than one stimulus[17 18 19]. This has attracted considerable attention from both academic and technological aspects[20]. A possibility to combine pNiPAM hydrogel or nanoparticles with other materials such as gold or magnetic particles clearly provides numerous new applications [21]. Thermoresponsive pNiPAM co-polymer (poly-N-isopropylacrylamide and – N,N-methylenebisacrylamide as a crosslinker) exhibits adjustment of the interactions between the polymer chains and the solvent media around the critical temperature. The phase transition as shown schematically in Fig. 1, and hence the origin of the 'smart polymer material' behavior comes from the entropic gain when water molecules associated with the side-chain isopropyl are released into the aqueous phase as the temperature increases above the critical point. A sharp coil-globule transition in water at 33^{o}C, changing from a hydrophilic state below this temperature to a hydrophobic state above it. The fact that this reversible transition, LCST - lower critical solution temperature lies close to the human body temperature which makes it particularly suitable for

biomedical applications. Above that LCST at 33°C in aqueous solutions [22,23] offers an important parameter for tuning the properties. The LCST is a widespread phenomenon among H-bonding sites containing polymers. In this class many others worth mentioning polymers such as N,N-diethylacrylamide (DEAAm), poly-N-vinylcaprolactam (PVCL), polyethylene glycol (PEG), polyethylene oxide (PEO) and polypropeleneoxide (PPO) exhibits an LCST which range is quite broad from 25°C up to 32°C. All of these polymers are water soluble and their solutions exhibits dramatic viscosity increase above the critical temperature (LCST), forming semi solid gels. Better understanding and tuning of these properties sure can expend the knowledge of a system which consequently will improve the practical applications. This approach allows looking at poly-N-isopropylacrylamide as a fine tunable model system with promising dye based bio-medical applications.

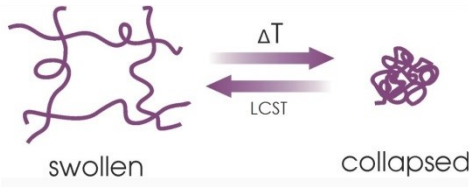

Figure 1: Scheme of pNiPAM network collapsing with temperature.

Combining the strengths of hydrogel and dispersion of nanoparticles, with unique stimuli-responsivity, pNiPAM microgels have found numerous biomedical

applications. Drug delivery which is perhaps the most well-known application is based on a simple idea that synthetic polymers are being used as a polymeric drug itself or in combination with small molecule drugs or with biomacromolecules such as proteins and nucleic acids. If the polymer is not a drug itself, it often provides a function as a drug carrier, reducing immunogenicity, toxicity or degradation, whilst improving circulation time and potentially a targeting function. In general these polymeric drug delivery systems can be divided into 5 subclasses: polymeric drugs, polymer-drug conjugates, polymer– protein conjugates, polymeric micelles and polyplexes (complexes of polymers and nucleic acids)[24]. This field is usually characterized by the terms 'polymer therapeutics' or 'nanomedicines'. Other uses of pNiPAM nanoparticles as biosensing, tissue engineering scaffolds, cell culture supports, bioseparation devices, sensors or actuators systems require same characteristics in terms of water-solublity, non-toxicity and non-immunogenicity but they are no longer based on simple dispersion of nanoparticles in a good solvent. PNiPAM nanoparticles can also be used as building blocks to fabricate 2D films and 3D aggregates which exhibits new properties, and new biomedical applications. Thus it is crucial to investigate not only dispersed particles but also nanostructured assemblies which consist of nanoparticles. Using a dye for probing a polymer network may open new way to study this structures with various fluorescent techniqes for its potencial bio-application [25]. Recent studies show that pNiPAM has even more interesting aplications as potencial biofilm for cells growth [26]. PNiPAM hydrogel can also

influence cell clutures by exhibiting unique growth patterns in *in-vitro* examination[27]. Studying these new approch for investigating new applications can be done by synthesising the well-defined pNiPAM NP's characterazing it and funcionatalizing it with fluorescent dye. A new bio imigaging nanoparticles with a potential appliction as a biosensor and a fine model system for studying single particles dynamics employing fluorescence techniques can surly be developed [28].

2. OBJECTIVES OF THE THESIS

The main objective of this work was to synthesize thermoresponsive pNiPAM nanoparticles for further potential application and to closely study the physico-chemical and biological properties of the system. That includes a detailed characterization of the system in terms of its thermo-responsibility, size and size changes with temperature, rheological properties of the polymer and finally its biocompatibility. In all these studies various experimental techniques will be used. Additionally, the nanoparticles will be functionalized by chemically incorporating a fluorescent dye into the nanoparticle polymer network. The functionalized pNiPAM nanoparticles will be used to study viscosity and crowded system dynamics by means of Fluorescence Correlation Spectroscopy.

3. MATERIALS AND METHODS

3.1. Chemical reagents

- N-isopropylmethacrylamide (NiPAM)
- N,N-methylenebisacrylamide (BIS)
- Sodium dodecyl sulfate (SDS)
- 2,2-azobis(2-methylopropioitrile) (AIBN)
- Fluorescein
- Fluorescein isothiocyanate isomer I (FITC)
- Allyl amine
- Tri-cyclohexyl carbodiimide (TCC)
- 1,4 – Dioxane

All the above listed substances were purchased from Sigma-Aldrich. As a general rule deionized milli-Q water of a specific resistivity of 18 MΩ/cm was used in all experiments.

Sample	NIPAM [mmol]	SDS [mmol]	BIS [mmol]	AIBN [mmol]	Fluorescein[1]/FITC allylamine hydrochloride[2]	Water [ml]
TD-1	44	0,52	0,44	0,484	-	100
TD-2	44	0,52	1,32	0,484	-	100
TD-3	44	0,308	0,44	0,484	-	100
TD-4	44	0,308	1,32	0,484	-	100
TD-6[1]	44	0,52	0,44	0,484	0,44	100
TD-8[2]	44	0,52	0,44	0,484	0,7	100

Table 1: Values of monomer, co-monomer, surfactant and initiator molar concentrations used for the synthesis.

3.2. *Synthesis of pNiPAM nanoparticles*

3.2.1. *Emulsion fre-radical copolymerization*

The aim was to synthesize water dispersible pNiPAM nanogel particles with various degree of cross-linking. The synthesis took place by emulsion free-radical copolymerization in water. The mixtures were prepared in 250 ml round bottom flask previously dried and were purged with nitrogen gas, 100 ml of nano-pure water were used for the synthesis. The surfactant SDS was first dissolved in nano-pure water to form micelles. Then NiPAM monomer, co-monomer BIS and initiator - AIBN in this order were added to the mixture. In order to get rid of all the oxygen from the vial mixtures were purged with nitrogen gas for 20 minutes. After this the polymerization was carried out under good stirring for 4 hours at 70° C using oil bath temperature control. After four hours the polymerizing mixtures were left to cool down with open access to air. The whole reaction mixture was purified to remove the unused surfactant and unreacted starting materials: the monomer, crosslinker and initiator. This was achieved by ultrafiltration, removing excess solvent and adding fresh solvent for at least 3 times.

3.2.2. *Reversible addition–fragmentation chain-transfer (RAFT) polymerization of linear pNiPAM chains*

The synthesis took place by Reversible Addition Fragmentation Transfer (RAFT) polymerization. The goal of my work was to synthesize the linear pNiPAM chains with various molecular weights. In order to get clean product first the NiPAM monomer had to be re-crystalized. The procedure of cleaning the monomer, meaning re-crystallization of NIPAM from Benzene-Hexane mixture starts with dissolving the monomer in a mixture of Benzene and Hexane in a ratio 1:3. Then the mixture was heated up to about 60°C (50-60°C) while stirring. Once the mixture started to crystallize again the solvent was removed with the pipette. Clear monomer was left under vacuum to dry completely. Before it was ready to use an extra filtration with a syringe filter was performed. During the polymerization exposure to air (oxygen and water) should be avoided. In order to do so the mixture was put 3 times in turns as following in: liquid nitrogen to freeze, vacuum line to get rid all the air for 10-15 min, Nitrogen pump as it was getting back to room temperature. Polymerization took place at 60°C for 24 hours, after this it was left to cool down in contact with air (opened). The product of the synthesis was precipitated in hexane by slowly adding droplets of the polymer mixture to an amount at least 10x more than hexane. After the precipitation of the liquid phase in hexane all the impurities were removed and the polymer was left to dry. This procedure was repeated at least 3 times. The product was characterized with H^1 NMR and GPC

The ratio between the components should be:

5(TCC): 1 (AIBN): 100 (NIPAM)

3.2.3. *Preparation of dyes for further functionalization*

3.2.3.1. Preparation of functionalized fluorescein

3g (9 mmol) of fluorescein were placed in a 250 ml round bottom flask followed by the addition of 80 mL of dry tetrahydrofuran (THF). Then 28 ml (207 mmol) of triethylamine (TEA) was added to bond the acid hydrogen and form a salt. All the components were mixed under a nitrogen flow and continuous stirring. Next, 2 ml (20mmol) of Acryloyl chloride was added while the reaction was kept in an ice bath. The reaction was allowed to proceed overnight before removing the excess of reagents under reduced pressure. The mixture was filtered with paper filters in order to remove the triethylammonium chloride salt produced. The nitrogen gas was pumped for about 5 min just before distillation process. The fluorescent cross-linker was dried under reduced pressure to retrieve the orange product which was characterized by ^{1}H NMR.

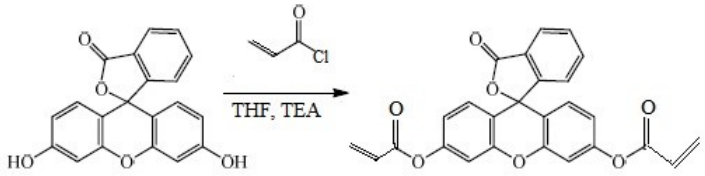

Figure 2: Reaction scheme for the synthesis of fluorescein cross-linker

3.2.3.2. Preparation of functionalized FITC

66 µl of allyl amine were placed in a 50 ml round bottom flask previously dried and purged with nitrogen gas, followed by the addition of 5 mL of dry tetrahydrofuran (THF). FITC was added to this mixture in order to bond the acid hydrogen and form a salt. All the components were mixed under a nitrogen flow and continuous stirring on ice bath. The reaction was allowed to proceed for 24h before removing the excess of reagents under reduced pressure. The fluorescent co-monomer was dried under reduced pressure to retrieve the orange product which was characterized by ^{1}H NMR.

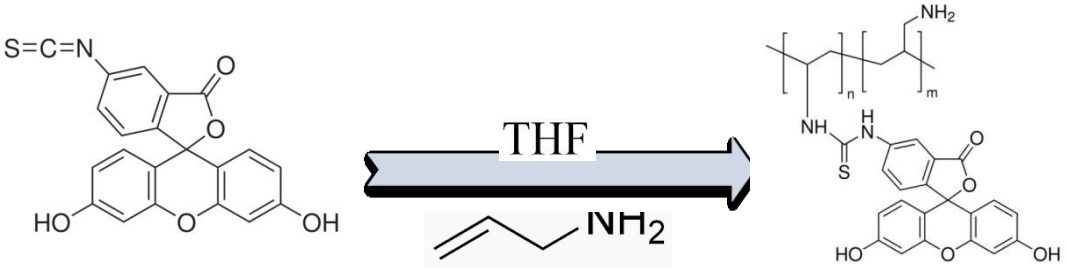

Figure 3: Reaction scheme for the synthesis of fluorescein isothiocyanate ally amine hydrochloride.

3.3. *Synthesis of Fluorescent pNiPAM*

The aim was to synthesize water dispersible pNiPAM nanoparticles labeled with fluorescent dye, incorporated in the polymer network: as a co-cross-linker (TD-6) and as a co-monomer (TD-8). The synthesis took place by emulsion free-radical copolymerization in water. We use two different approaches which are presented below: *a)* Introducing fluorescein as a cross-linker which allows controlling the

degree of dye incorporated in the particle and *b)* using functionalized FITC as a co-monomer which also allows controlling the degree of dye content in the particle and additionally doesn't affect the synthesis process.

3.3.1. *Purification of Fluorescent pNiPAM*

In order to separate unwanted fluorescent compounds from pNiPAM nanoparticles in solution a selective and passive diffusion through a semi-permeable membrane were employed. To remove the excess of fluorescent dye sufficient the dialysis using 3ml Slide-A-Lyzer MINI Dialysis Devices with 10K MWCO took place for at least 48h. To control the process of purification and compere the two approaches of dye incorporation fluorescence correlation spectroscopy technique (FCS) was used, which is commonly used to study the self-diffusion of fluorescently labeled molecules at a single molecule resolution.

3.4. Physico-chemical characteristics of nanoparticles

3.4.1. *Dynamic Light Scattering characterization*

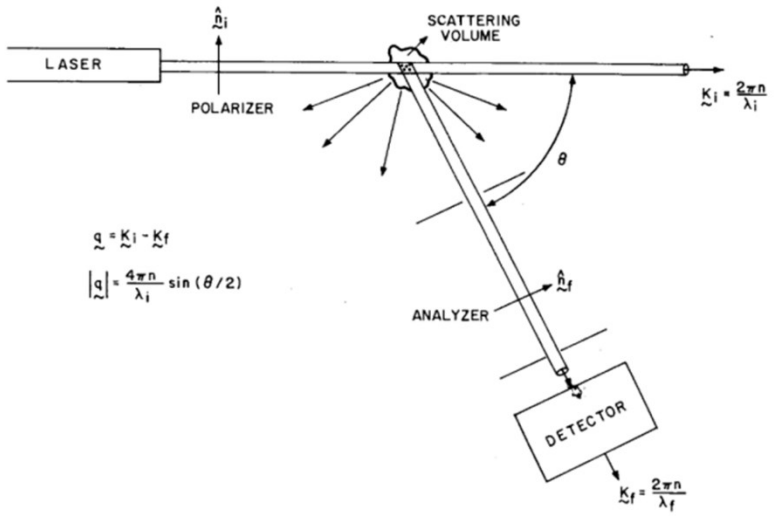

Figure 4: Schematic diagram of the setup for dynamic light scattering experiments with polarization vectors and scattering angle Θ shown.

Light scattering techniques are used in many different laboratories for determining the sizes of nanoparticles in solutions. The phenomenon of light scattering was first studied and described by Tyndall [29]and then developed by Lord Rayleigh [30]. Scattered light intensity I_s is inversely proportional to the fourth power of the wavelenght of the electric field of the incident light E_s thus:

$$\frac{I_s}{I_0} \sim \frac{16\pi^4\alpha^2}{\lambda^4 r^2}$$

Equation 1

Where α is a tensor of optical polarity of the scattering molecule. In suspension the micro/nano particles, which are much bigger than the solvent particles, mostly contribute to the fluctuations of the scattered light coming from the suspension. These fluctuations are due to results from translational and rotational diffusion of the nanoparticles and their interactions. The dynamic information about the particles is derived from an autocorrelation function of the intensity trace recorded during the experiment.

$$g^{(2)}(q;\tau) = \frac{\langle I(t)I(t+\tau)\rangle}{\langle I(t)\rangle^2} = 1 + B\left|g^{(1)}(\tau)\right|^2 = 1 + B\left|\exp(-\frac{t}{\tau_R})\right|^2$$

Equation 2

Where, $g^{(1)}(\tau)$ and $g^{(2)}(\tau)$ are the first and second order correlation functions, respectively, τ is a delay time, τ_r is the relaxation time, ***I*** intensity and ***q*** is a wave vector. The translational diffusion coefficient *D* can be derived at a single scattering angle or at a range of angles, since:

$$\tau_R = \frac{1}{q^2 D}$$

Equation 3

And the length of the scattering vector:

$$q = \frac{4\pi\eta_0}{\lambda}\sin(\frac{\Theta}{2})$$

Equation 4

Where **λ** is the incident laser wavelength, n_0 is the refractive index of the sample and *Θ* is the scattering angle. The most reasonable method to analyze the correlation function of polydisperse systems with sufficiently narrow size

distribution is the cummulant method. In this method the correlation function is analyzed in the following form.

$$g^{(1)}(q,\tau) = \exp(-\acute{\Gamma}\tau)(1 + \frac{\mu_2}{2!}\tau^2 - \frac{\mu^3}{3!}\tau^3 + \cdots)$$

Equation 5

The value of the translational diffusion coefficient D is used to calculate the hydrodynamic radius (R_h) of a sphere through the Stokes–Einstein equation.

$$D = \frac{k_B T}{6\pi\eta R}$$

Equation 6

Where k_B is the Boltzman constant, T is the absolute temperature and η – viscosity of the solvent.

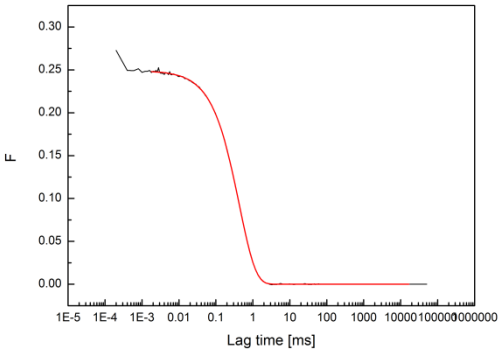

Figure 5: Typical DLS correlation function (black line) and the fit (red line).

The hydrodynamic radius of the polymeric nanoparticles in dilute regime (nanomoles) in water was measured by dynamic light scattering (DLS) using the green laser at a wavelength of 532 nm as the light source and the ALV-5000/E digital correlator. The scattering intensity was measured at 5 different angles (30°, 45°, 60°, 90°, and 150°) and a range of temperatures from 20 to 38°C for each

sample. The time for each measurement was 200 seconds. The resulting 1-st order correlation functions were fitted using cumulant method *(eq.5)* and CONTIN algorithm in order to calculate the mean diffusion coefficient D of the suspended particles. The hydrodynamic diameters 2R were calculated from the Stokes-Einstein - equation 6. The concentrations of solutions for light scattering experiments were chosen in such a range that the measured size did not depend on concentration. Once an approximate concentration range of the dilute regime is established all subsequent measurements were performed at a single concentration. The samples were also *sonicated* in order to dissolve the potential aggregates of particles.

3.4.2. Particle Tracking

In the particle tracking (PT) experiments the particle displacement x is measured as a function of time and the self-diffusion coefficient D_s is calculated using the equation:

$$< x^2 >= 2kD_s t$$

Equation 7

where k is the dimension of the space. Usually in the experiments a microscope objective is used and the projection of the particle position on the confocal plane is measured, thus k=2. The values of the hydrodynamic radius of the pNiPAM nanoparticles obtained from the DLS measurements were compared with the

corresponding data obtained from NanoSight NS500 measurements using Nanoparticle Viewing Unit at temperatures of 20, 25, 30, 35, and 38°C. Using particle tracking (PT) setup, additional DLS measurements were performed at 86° angle to investigate the particle size and the size distribution.

3.4.3. *Fluorescence Correlation Spectroscopy*

Fluorescence correlation spectroscopy was first introduced as a method for diffusion coefficients and concentration measurements. The method itself is based on measuring the diffusion of single fluorescent molecules which are passing through the confocal volume. Obviously many modifications to the method have been presented along it development but the principle of the measurement remains the same. Frequently FCS method is still used to measure the self-diffusion coefficient of fluorescently labeled probes in solutions, complex media, and living cells. The FCS experiment itself measures spontaneous intensity fluctuations which can be quantified in their strength and duration by temporally autocorrelating the recorded intensity signal. The correlation functions (CFs) is being analyzed in a standard form:

$$G(\tau) = \left[1 - T + T\exp(-\tau / \tau_T)\right] \frac{1}{N(1-T)} \frac{1}{1 + (\tau / \tau_D)} \left(\frac{1}{1 + (\tau / \tau_D)(\omega_0 / \omega_z)} \right)^{1/2}$$

Equation 8

Whwhere T is the so-called triplet fraction, τ is the diffusion time of NPs, τ_T is the characteristic time of the triplet contribution, τ_D is the translational diffusion time,

N is the number of particles in the confocal volume and ω_0 and ω_z are axial and longitudinal measures of the Gaussian point Spread Function.

The idea behind the FCS experiment is to quantify the magnitude and duration of fluorescence fluctuations coming from fluorescently labeled probe diffusing in the measured volume called confocal volume. In an ideal sample the number of the particles in the measured volume is of the order of one and knowing the size of confocal volume one can calculate the characteristic time the particles take to cross confocal volume. This time is proportional to the square of the radius of the confocal volume σ. Knowing the size of the confocal volume the translational self-diffusion coefficient of the fluorescent probe can be calculated. To study fluorescent nanoparticles, the Zeiss ConfoCorIII instrument equipped with the LSM 780 NLO confocal microscope was used. Argon-ion laser with low power was used to excite the dye at 488 nm.

3.4.4. *Scanning Electron Microscope*

3.4.4.1. SEM

To investigate the size and shape of the nano-particles the Scanning Electron Microscope Jeol 7001TTLS was used. For scanning electron microscopy imaging of micrographs the accelerating voltage of 15 kV and secondary electron (SEI) mode was used. pNiPAM NP's were deposited on a glass plate and dried out of solution (concentration as for the light scattering experiments) and coated with platinum

using a sputtering system (Quorum Technologies PP3000T) for 60 seconds to provide an electrically conductive thin film.

3.4.4.2. Cryo-SEM

The morphology of the synthesized samples was assessed by performing a cryo scanning electron microscopy, Cryo-SEM (Jeol, JSM 7001F TTLS). For scanning electron microscopy imaging of micrographs the accelerating voltage 15 kV and secondary electron (SEI) mode was used. Samples of a high concentration (1 g of stock solution, see *Table 1,* in 1 ml of water*)* were deposited on a glass plate and rapidly frozen in liquid nitrogen and coated with platinum using a sputtering system (Quorum Technologies PP3000T) for 60 seconds to provide an electrically conductive thin film to reduce thermal damage and charging of the samples.

3.4.5. Rheology

Rheology (from Greek *rhéō*, "flow" and, *-logia*, "study of") is the study of the flow of matter. Rheological properties of a particular system are based on the response to an applied force. Primarily in response to applied force one can distinguish flow for liquids and deformation for solids. Within solids elastic (return to relaxed shape after applied stress) and plastic (deformed permanently after applied stress) response can be observed while liquids flow as Newtonian fluids (strain rates proportional to applied stress) or Non-Newtonian (strain rates is not proportional to applied stress). However many of the real-life materials do not fit

in this scheme that obviously. For example a group called 'soft-matter' present viscoelastic behavior and they are substances which have a complex microstructure, for instance polymers. Viscoelasticity can be easily explained by the Rouse-Zimm model where the single chain diffusion is represented by Brownian motion of beads connected by harmonic springs and thus the entangled polymer chains can be analyzed with two different approaches. Polymers chains are considered to be made out of spheres/beads connected by harmonic springs. Thus, both the viscosity and elastic modulus can be seen. To study this kind of system response a oscillatory frequency sweep measurements had to be taken. Once we applied a sinusoidal deformation force – strain γ:

$$\gamma = \gamma_0 \sin \omega t$$

Equation 9

Where

γ_0 – strain amplitude

ω - oscillation frequency

A stress is being created in the sample.

$$\tau = \tau_0 \sin(\omega t + \delta)$$

Equation 10

Where

τ_0 - stress amplitude,

δ - phase shift

To represent the relations between the oscillating stress and strain, **G'** (storage modulus) and **G''** (loss modulus) have to be introduced.

$$G' = \frac{\tau_0'}{\gamma_0}$$

Equation 11

$$G'' = \frac{\tau_0''}{\gamma_0}$$

Equation 12

The oscillatory rheological experiments are extremely useful because viscoelastic responses of the system are based on short time dynamics. Results are being analyzed by the storage and loss modulus thus the strain amplitude is proportional to the stress amplitude (Equation 11). To probe the properties of the material a well-defined force is being applied and the deformation is measured. The linear and non-linear response properties of previously synthesizes hydrogels (*see Table 1)* were studied using strain-controlled rheometer (ARES 100FRTN1 from TA, USA). Measurements were performed with a titanium cone-and-plate geometry (25mm diameter and 0.04 rad cone angle). The temperature was controlled with Peltier Module operating with a recirculating water/ethylene glycol bath. The pre-shear strain of 100 % was applied for 600 second to fluidize the sample and to restore reproducible initial conditions before the measurements [31]. All the samples were measured on the rheometer applying the same protocol. Dynamic strain sweep test were performed at 1 rad/s frequency with a strain range 0.1-200% and

dynamic frequency sweep were performed with strain of 1% in a frequency range 100-0.5rad/s. To minimize sample evaporation a self-made trap was employed.

3.4.5.1. Viscosity measurements

Antoher useful parameter in therms of polymer nanopoarticles solutions characterization is its viscosity. In practice viscosity is being measured at multiple concentrations of a dilututе solution then is extrapolated to zero concentration. This is an important characterization method especially for polymers in solutions because viscosity is proportional to the volume of a polymer coil or globule (Fox-Flory), making it a crutial parameter for investigating volume fraction of a polymer solution. The volume fraction of the nanogel particles in water was determined from the viscosity measurements of pNiPAM suspensions with varying particle concentration. Viscosity measurements were performed on suspensions in the concentration range $0 < C < 0.20$ g/cm^3 at 20+/-0.1°C using Anton Paar DMA 4500M instrument. The experiment was performed in the dilute concentration range and the data were analyzed using the Einstein relation with the Batchelor's correction (E*q.13*) for particle-particle interaction effect.

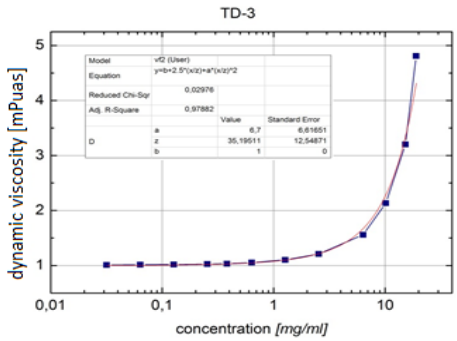

Figure 6: Einstein-Batchelor fit of dynamic viscosity for zero-shear viscosity.

$$\eta(r) = 1 + 2.5\,\phi + 6{,}7\,\phi^2$$

Equation 13

3.5. *Biocompatibility tests*

3.5.1. Preparation of cell lines

Examination of cytotoxicity was conducted on HeLa (cervical cancer cell line) and HeK293 (human embryonic kidney cell line) cell cultures, which were cultured in DMEM (Dulbecco's modified Eagle's - Sigma) containing 10% FBS (fetal bovine serum - Gibco Invitrogen) supplemented with antibiotics (penicillin 100 µl/ml, streptomycin 100 µg/ml - Gibco Invitrogen) and incubated in humid atmosphere, 5% CO_2 at 37°C. When the culture reached needed confluence, cells were trypsinized (trypsin - Gibco Invitrogen) and seeded on culture plates. For the tests, first, HeLa cancer cell line was selected mainly due to its durability and fast proliferation. Secondly, HEK293 cell lines were employed since their proliferation is fast but they do not possess cancer cell line features.

3.5.2. MTT test

MTT (dimethylthiazol biphenyl tetrazolium bromide) is a colorimetric assay (from Roche) for assessing cell viability. Measurement of the absorption of formazan at a wavelength of 572 nm reflects the number of metabolically active cells and is based on cleavage of the yellow tetrazolium dye (MTT) to purple formazan by metabolic active cells. Cells were seeded in 96-well plate at conditions described above, and then were cultured to 70% of confluence before adding the nanogel. In order to get different pNiPAM hydrogels solutions, 50 to 2000 µg of the stock solutions were dissolved in 1 ml of ultrapure (type 1) water (Merck *Millipore* Milli-Q® *Water*), see *Table 1* (50, 100, 200, 500, 1000, 2000 [µg/ml])**.** Each solution was added to 3 wells for cell viability test plus negative probe with dimethyl sulfoxide (DMSO) and, respectively, three positive probes (cells with no NPs added) were analyzed each time. Cells were cultured in an incubator at 37°C and 5% CO_2 in a humid atmosphere for 24 and 48 h in the presence of pNiPAM nanoparticles. After the incubation time 10 µl of MTT (0.5 mg/mL) were added. The formazan crystals were then dissolved in DMSO and the plate was incubated at 37°C for 4 h. The optical density (OD) was read with multiwell microplate reader (Zenyth) at 570 nm.

3.5.3. Viability test

Cell viability test – measured by Muse® Cell Analyzer: Mini, Affordable Flow Cytometry (Muse Count & Viability Assay Kit Merck Millipore). Cells were seeded on 12-well plate at conditions described above, and then were cultured to 70% confluence before adding the nanogel. In order to obtain different pNiPAM

hydrogels solutions, 50 to 2000 µg of the stock solutions were dissolved in 1 ml of ultrapure (type 1) water (Merck *Millipore* Milli-Q® *Water*), see *Table 1* (50, 100, 200, 500, 1000, 2000 [µg/ml]). Each solution was added to 3 wells for: cell viability test plus negative probe with dimethyl sulfoxide (DMSO-10%) and, respectively, three positive probes (cells with no NPs added) were analyzed. Cells were cultured in an incubator at 37°C and 5% CO_2 in humid atmosphere for 24 and 48 h in the presence of pNiPAM nanoparticles. Then, the medium was removed and cells were harvested in 0.2 ml trypsin-EDTA solution (0.25% trypsin, 0.02% EDTA). Then, cells were treated with Muse Count & Viability Assay Kit according to manufacturer's description (Merck Millipore).

3.5.4. *In-vitro* analysis of fluorescent pNiPAM NP's used in range of concentration

To confirm direct cell growth on pNiPAM, first we coated 96-well plates by adding 50 µl of pNiPAM NPs (doped with FiTC dye) solutions which were added for each well with given concentration. After one hour of incubation (enabling drying) HeLa and HEK293 cell lines were seeded for 24h at conditions described above. Medium was then removed and cells were stained with Hoechst33258 blue fluorescent dye for DNA of the nuclei of HeLa and HEK293 cells. Images of HeLa and HEK293 cell cultures grown on a pNiPAM coated surface were obtained by means of the IN Cell Analyzer 2000 automated cellular and subcellular imaging system. Finally the same concentration of pNiPAM NPs (1 g of stock solution, see Table 1, in 1 ml of water) as for the Cryo-SEM investigation were used.

3.5.5. *Statistical analysis*

In order to obtain statistically relevant data from both MTT and cell viability test, three independent probes were taken into account each time. Additionally independent t-test for each probe with differences established at $p<0.05$ ($p=0.0408$, standard deviation ~5%) was used to verify statistical significance.

4. RESULTS AND DISCUSSION

4.1. Synthesis of various types of pNiPAM

As a result of the synthesis six different types of pNiPAM hydrogel nanoparticles (TD-1, TD-2, TD-3, TD-4, TD-6, and TD-8) were synthesized. Since it is crucial for the synthesis to be well controlled and at the same time keep it costs low, a well-defined method has been chosen. Emulsion free radical copolymerization in water is a well-known method and it was selected mainly because of good control of a product in terms of various sizes, swelling ratios and volume fractions of pNiPAM NPs (see table 2). It was previously shown that among many different synthesis methods, co-polymerization or salt concentration manipulation, emulsion free radical polymerization allows easier and well-control synthesis that can deliver desirable particles [32]. Among many applications of the pNiPAM particles the majority is clearly size dependent. The particle size should be in µm-size range in order to be visible in optical microscopy experiments. Introducing new characterization methods one can easily 'see' particles bigger than 30nm using light scattering, fluorescence or lately even particles tracking methods. Herein a simple and well-known synthesis method is presented. The pNiPAM NPs achieved allows studying large ratio of particle sizes with different interior architecture which influences the properties for dynamics studies and biocompatibility studies. (Table 2).

4.2. Characteristics of pNiPAM nanoparticles

As mentioned before during the past decade many methods that allow the preparation of polymeric nanoparticles with varied and complex structures and functions have drawn much attention. This interest is largely based on the fact that such nanoparticles in the size range from tens to hundreds nanometers may offer enhanced physical, chemical, or biological properties when optimally designed for specific applications. Development of any potential commercial application requires reproducibility in relatively high volumes and at costs commensurate with the value of the benefit they are expected to impact in different applications. The development of economically viable processes capable of producing desired nanoparticles has been a topic of numerous studies. It is important to use a synthesis method that can be well-controlled and at the same time learn more about control mechanism of the process. One needs a detailed characterization of the NPs in terms of physical, chemical properties and their application potential. However, what seems crucial for this and other synthesis methods are particles sizes. The size of the NPs is an important determinant for the kinetics and architecture of a single particle furthermore it determines the pathway of an uptake and route of delivery of the particle to the targeted area (cell or tissue). Size of a polymeric particle can be influenced by parameters such as initial monomer concentration, temperature and initiator concentration which in this case stays the same for all the synthesized nanoparticles. Additionally, the size is restricted by the monomer-to-surfactant and monomer-to-crosslinker ratio which both were

Sample	Surfactant SDS	Cross-linker BIS	Weight Concentration [mg/g]	volume fraction [ζ]	Swelling Ratio	Size R_h		Mesh size [nm]	Zeta potential
						20 - 22°C	34-36°C		
TD-1	1,2 mol%	1 mol%	12.7	0.69	2,4	72	54	4,6	-3,4
TD-2		3 mol%	13,6	0.72	2,3	58	44	2,8	-19,5
TD-3	0,7 mol%	1 mol%	14,5	0.78	5,6	94	53	3,9	-1,4
TD-4		3 mol%	10	0.45	3,3	77	52	3,1	-4,3
TD-6	1,2 mol%	1 mol%	-	-	2,5	110	81	5,8	-5,1
TD-8			-	-	3,7	82	53	3,4	-4,5

Table 2: Table with combined information about the synthesized pNiPAM NP's.

adjusted for achieving different nanoparticles diameters. As it can be seen in table 1 two different monomer-to-surfactant and monomer-to-crosslinker ratios were selected.

4.2.1. Size

For typical reaction conditions particle size is restricted to diameters around hundreds of nm thus characterization of nanoparticles first required their nano-size confirmation. Since pNiPAM forms a hydrogel which means that synthesized nanoparticles are suspended in solutions (in water) one can determine the size of nanoparticles in solution using light scattering techniques. This technique that is based on light scattering phenomena is quite unique among many different

techniques (NMR, neutron scattering or X-Ray) due to its ability to study the polymer solution in non-disturbed environment in hydrodynamic equilibrium. Thus, the light scattering techniques in recent decades became the technique of choice for size characterization in biology or chemistry labs. Moreover since the basics of the theoretical approach are well developed this experimental approach is getting effectively more and more accurate in terms of size, shape and size distribution determination[1].

4.2.1.1. Dynamic Light Scattering

As a result of dynamic light scattering experiment, six pNiPAM water-soluble nanoparticles with various sizes were determined (*see table2*). As expected the diameter of synthesized nanoparticles in general depend on crosslinker-to-monomer ratio and as this ratio droped to 1% for TD-1, TD-3 and TD-6 the particles are slightly bigger.

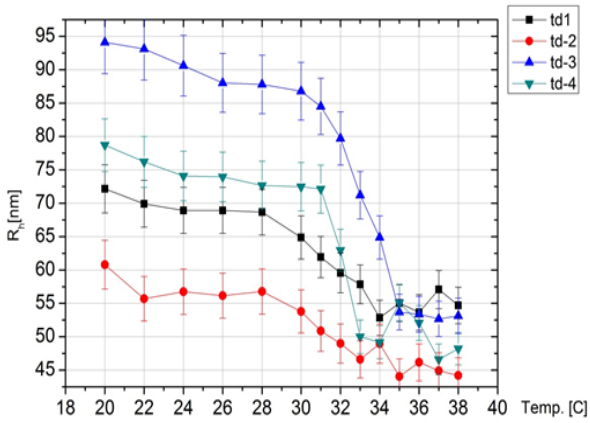

Figure 8: Hydrodynamic radius measured with DLS as a function of temperature.

Similar effect can be seen with adjusting the surfactant-to-monomer ratio where lower amounts of the SDS used resulted in a smaller nanoparticles diameter what can be seen for TD-3 and TD-4 in comparison to TD-1 and TD-2. Nevertheless, a sharp decrease in hydrodynamic radius of pNiPAM polymer when approaching 33°C for all synthesized nanoparticles, confirms system temperature response. This typical response due to the lower critical solution temperature (LCST) is a phase transition from a swollen hydrated state to a shrunken dehydrated state, in which NP is losing most of its volume. LCST is a unique and characteristic property of the system which exhibits hydrophilic interactions when the temperature is below the LCST and as the temperature increases the hydrophobic interactions become more favorable and the polymer network collapses which appears as a decrease in the particle size (*Fig. 8*). Similar transition occurs in biological systems such as proteins where expanded coil transforms finally into collapse globule. Since pNiPAM NPs collapse and expels its liquid contents at a temperature near the human body temperature it is truly a promising material with a wide spectrum

of potential applications. Based on hydrodynamic radius measured at low (20-22°C) and high (34-36°C) temperature the swelling ratio was calculated as a ratio of the volume of the swollen polymer network and the collapsed one. Since pNiPAM is a thermoresponsive polymer its volume fraction change is due to the change of its hydrodynamic radius. As one can see in Table 2 the swelling ratio and the volume fraction are increasing with decreasing SDS concentration and decreasing crosslinker concentration. More detailed explanation and analysis on nanoparticles volume fraction will be given in a separate paragraph. In terms of potential industry use as a drug carrier –drug delivery system (DDS) the capability of loading and releasing the potential drug is important. The mesh size (presented in *Table 2*) of swollen network of nanocarriers which is an important property for designing the DDS based on thermos-responsive pNiPAM nanogels were checked. First, the distance between two crosslinking points for unswollen nanogel was calculated using *equation 14*[33].

$$r = l[\frac{2M_c}{M}]^{1/2} C_N^{1/2}$$

Equation 14

Where:

r - the distance between two crosslinking points in the unswollen gel

l - the length of a C–C single bond (L=0.154 nm)

M_c - the molar mass of the polymer fragment between two crosslinking points

M - the molar mass of the monomer

C_N - the characteristic ratio, a measure of the extension of the polymer chain in a disordered condition (for acrylates: 6.9) [34].

Then the molar mass between two crosslinking points was calculated from

$$M_c = \frac{n(NiPAM)}{n(BIS)}\, M(NiPAM) = M(BIS)$$

Equation 15

M(NiPAM) - the molar mass of NIPAM (113.18 g/mol)

M(Bis) - is the molar mass of Bis (154.17 g/mol)

n(NiPAM) - the used molar concentration of NiPAM

n(Bis) - the used molar concentration of Bis.

As a result one can determined the mesh size- ξ of the swollen nanogel network using:

$$\boldsymbol{\zeta = \frac{r}{v_{2m}^{1/3}}}$$

Equation 16

Where:

v_{2m} - value of the swelling degree

r - the distance between two crosslinking points in the unswollen gel.

4.2.1.2. Particle tracking analysis

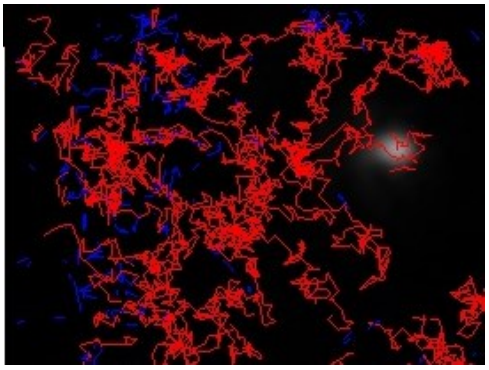

Figure 8: Tracks of pNiPAM NP's measured with NanoSight NS500 particle tracking method.

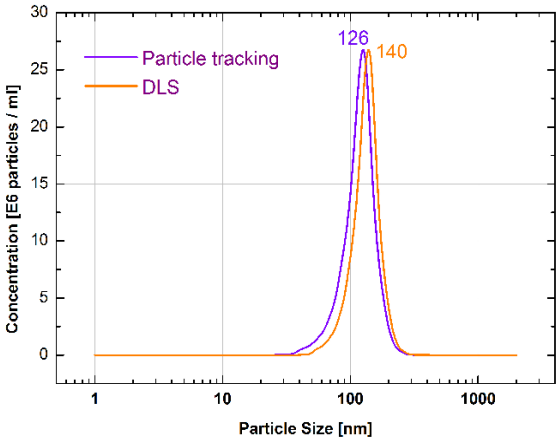

Figure 9: Plot from NanoSight NS500 (PT) presenting size of particles measured with the particle tracking method.

Another approach which is using light scattering phenomena is the particle tracking analysis (TA) conducted by Nanosight (Marveln) instrument. With this set-up one can perform quick and simple analysis of nanoparticles size and size distribution. The used concentration of the sample stays in a range of picomoles. Using the same instrument the DLS measurement at the scattering angle at 86^{o} can also be performed. Particle tracking experiment was performed to compere results from the two techniques. What can be seen in *figures 8 and 9* is a result of measurements using the NanoSight instrument. The black line on the plots represents particle tracking data and, respectively, the purple one – the DLS data. In figures *10-13* one can see the particles diameter determined from the diffusion coefficient using Stokes-Einstein equation measured with light scattering standard ALV set-up (DLS) and DLS and particle tracking (PT) using the NanoSight NS500. The results of the measurements by means of these three techniques were

plotted and the data are also presented in the table below (*Table 2*). The hydrodynamic radius of the pNiPAM particles measured with both dynamic light scattering instruments is higher than that obtained from PT for all the particles. This is consistent with our expectations because DLS measures the D_z value and PT measures the corresponding D_n value (*Eq.18 and 20*) and $D_z<D_n$, thus $R_z>R_N$. This difference varies from 10% (td4) up to 30% (td3) and depends on the polydispersity of the sample. The polydispersity of the presented pNiPAM nanogels is a result of two main mechanisms:

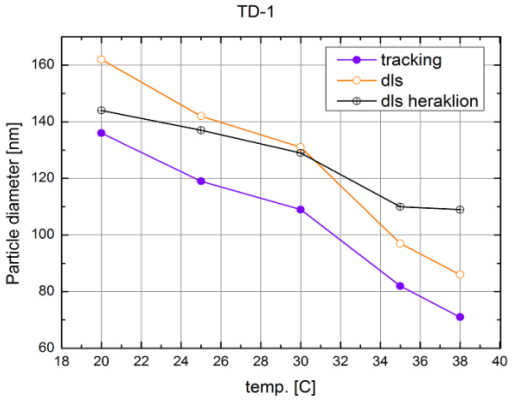

Figure 10: Particle diameter determined by three different techniques for TD-1 sample

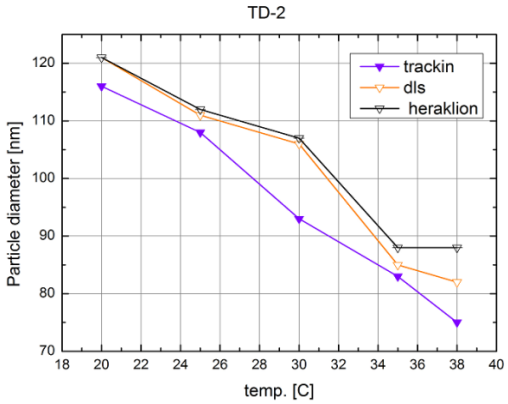

Figure 11: Particle diameter determined by three different techniques for TD-2 sample

1. Size distribution which is a result of the free radical emulsion polymerization process
2. Particle aggregation, which is considered to be caused by too high particles concentration and can be eliminated by diluting the sample.
3. Different swelling resulting from different crosslinking density

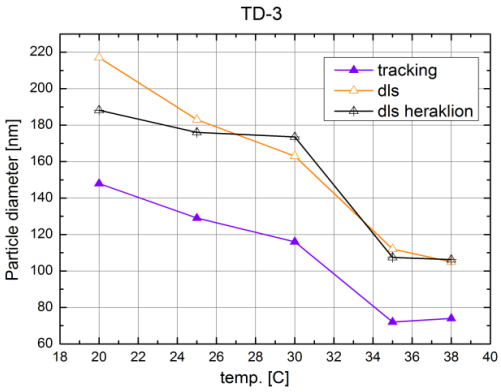

Figure 12: Particle diameter determined by three different techniques for TD-3 sample

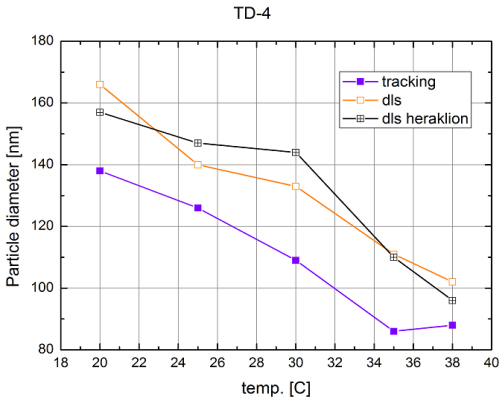

Figure 13: Particle diameter determined by three different techniques for TD-4 sample

Using light scattering techniques (DLS) it is crucial to understand that the intensity of scattered light depends on molecular weight of the particle and the mean diffusion coefficient is the so-called z-average defined by Eq.17. In the Particle Tracking Analysis (TA) we obtain particles size information based on the Brownian motion of individual particles and molecular weight distribution has no impact on sizing accuracy. In the TA the number average diffusion coefficient D_n given by Eq.19 is obtained.

Standard DLS method

$$D_z = \frac{\sum N_i M_i^2 D_i}{\sum N_i M_i^2} = \frac{\sum C_i M_i D_i}{\sum C_i M_i}$$

Equation 17

D_z – mean diffusion coefficient obtained calculated from DSL measurements

N_i – number concentration of fraction *"i"* of particles

M_i - molecular weight of fraction *"i"*

D_i – diffusion coefficient of fraction "i"

D_n – number average diffusion coefficient obtained from using NanoSight PT measurements

$$D_i = \frac{\Gamma_i}{q^2}$$

Equation 18

Particle tracking method

$$D_n = \frac{\sum D_i N_i}{\sum N_i}$$

Equation 19

$$D_n > D_z$$

Equation 20

$$R_n < R_z$$

Equation 21

Temp.	TD-1				TD-2			
	NANOsight		DLS	difference	NANOsight		DLS	difference
[°C]	TA	DLS		[%]	TA	DLS		[%]
20	136	162	144	16.0	116	121	121	4.1
25	119	142	137	16.2	108	111	112	2.7
30	109	131	129	16.8	93	106	107	12.3
35	82	97	110	18.3	83	85	88	2.4
38	71	86	109	17.4	75	82	88	8.5
Temp.	TD-3				TD-4			
	NANOsight		DLS	difference	NANOsight		difference	DLS
[°C]	TA	DLS		[%]	TA	DLS	[%]	
20	148	217	188	31.8	138	166	16.9	157
25	129	183	176	29.5	126	140	10.0	147
30	116	163	173	28.8	109	133	18.0	144
35	72	112	107	35.7	86	111	22.5	110
38	74	105	106	29.5	88	102	13.7	96

Table 3: Combined results from DLS and TA measurements.

4.2.1.3. Scanning Electron Microscope

Scanning electron microscope was used to confirm the spherical shape of the NP's. The separated nanogel particles pictures and a cluster of particles are presented below. As it can be seen in the figures 14, 15 and 16 pNiPAM nanoparticles are forming uniform spheres with a smooth surface. They appear in SEM pictures both as separate, doublets and clusters. The diameter obtained from SEM is consistent with light scattering results and for collapsed particles seen in SEM it is around 110nm for TD-2 and around 140nm for TD-3.

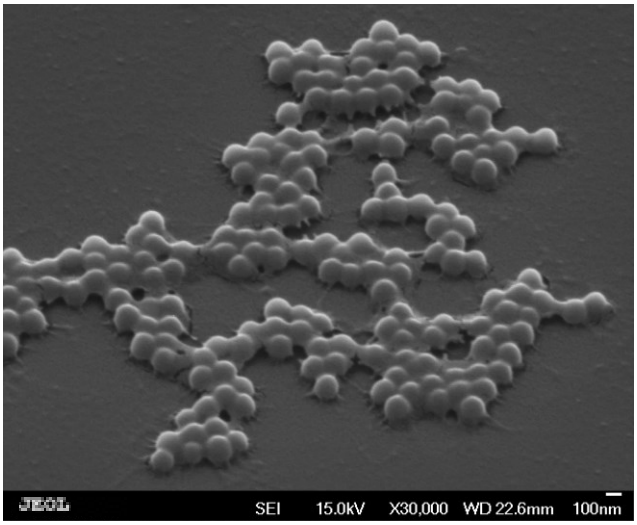

Figure 14: TD-3 sample, cluster of nanoparticles.

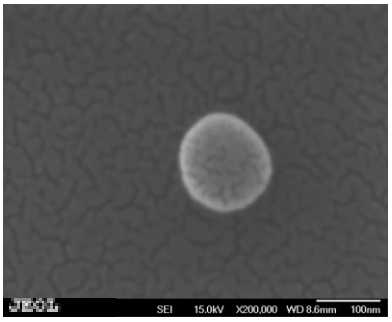

Figure 15: Single TD-2 NP.

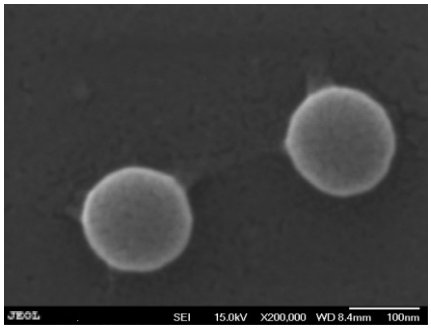

Figure 16: TD-3 NP doublet.

4.2.1.4. Fluorescence Correlation Spectroscopy (FCS) study

4.2.1.4.1. Efficiency of the fluorescent labeling of the pNiPAM nanoparticles

Detailed information concerning the efficiency of fluorescent labeling of nanoparticles (NPs) and on fluorescent properties of a single NP can be obtained from FCS experiment. In particular this experiment provides us with the value of the counts per molecule (CPM) at given excitation level and allows to separate the fluorescence signal coming from fluorescently labeled NPs from that coming from the remaining free dye (labeled monomer) solution and adsorbed to the NP but not chemically bound. In the latter case extensive dialysis of the sample at low (nanomolar) concentrations allows to completely remove this component. Such detailed characteristics of the fluorescently labeled NPs cannot be obtained from

fluorescent measurements using a fluorimeter. Here FCS was used to estimate and compare the fluorescence efficiency of two kinds of the fluorescent pNiPAM NPs: TD-6 and TD-8, prepared in a different way. First the excess free dye/monomer was removed from solutions by extensive dialysis. The amount of the free dye in solution was checked after each dialysis step by measuring the FCS correlation function (CF). The CFs were analyzed assuming the two component model, where fast component corresponds to the free dye and the slow one – to the NP.

$$G(t) = 1 + \frac{1}{N}\left[\frac{T}{1-T}e^{-t/\tau_T}\right)\sum_{i=1}^{2}\frac{A_i}{(1+\frac{t}{\tau_i})\sqrt{1+c^{-2}t/\tau_1}}\Bigg]$$

Equation 22

Where T is the so-called triplet fraction and τ_T is the characteristic time of the triplet contribution, N is the number of particles in the confocal volume, τ is the diffusion time of NPs, and $c = \sigma_z/\sigma_x$ is the aspect ratio of the Gaussian confocal volume. Before the dialysis the CFs were dominated by the contribution of the free dye, Fig 23 and the contribution of the NPs was hardly visible. The dialysis was performed until the NPs contribution dominated the CF. After the dialysis the count rate (CR) of the TD-8 sample decreased from $42x10^3$ to $25x10^3$ counts/s while the CPM remained constant at $25x10^3$counts/s. For the TD-6 sample the CR decreased from $83x10^3$ to $55x10^3$counts/s and the CPM decreased from $9x10^3$ to $5x10^3$counts/s. These changes indicate that a substantial part of the samples purified after synthesis in the usual way was due to the free dye adsorbed and not

chemically bound to the NPs. Since the CPM of the TD-8 sample was much higher than that of TD-6, it is clear that the synthesis of fluorescent pNiPAM NPs in which the fluorescently labeled co-monomer was used , results in NPs of higher fluorescent efficiency (TD-8) than in the case when fluorescent co-crosslinker was used (TD-6).

4.2.1.4.2. Micro- and macro-viscosity in crowded pNiPAM systems

Interesting information about the solvent permeability of NPs and the crowding effect can be obtained from the measurements of the probe-size dependent viscosity by means of FCS. From the value of the self-diffusion coefficient D_s measured by FCS one can obtain the viscosity η using the Stocks-Einstein relation (see Eq. 6). Where *R* is the radius of the fluorescent probe. It has been shown[35] that in crowded systems the viscosity "felt" by probes of different sizes changes from the viscosity close to that of solvent, for the smallest probes, to macroscopic solution viscosity, for probes of sizes exceeding some characteristic length of the crowded system. In order to learn more about the diffusion process in solutions of different pNiPAM NPs (TD-1 toTD-4, table 2) in a broad concentration range, we have measured the diffusion (viscosity) of a small probe – Alexa 488 and a large probe- fluorescently labeled pNiPAM NP (TD-8) in these solutions by means of FCS. The diffusion times obtained from these measurements as a function of the pNiPAM concentration in the range from 0 to 5000 μg/ml are shown in Figure 17 together with the macroscopic viscosity measured by rheological methods.

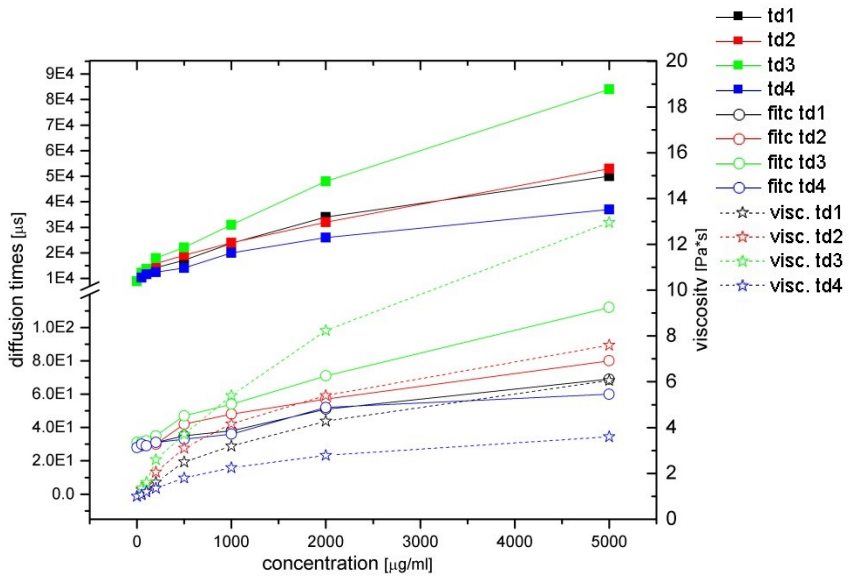

Figure 17: Diffusion times measured for Alexa488 –open symbols and solid lines, TD-8 filled symbols and solid lines and macroscopic viscosity –stars and dashed lines measured for solutions of pNiPAM: TD-1, TD-2, TD-3 and TD-4.

In Figure 17 one can see that the highest increase of the diffusion times of Alexa 488 and TD-8 NP as well as the macroscopic viscosity is observed in TD-3 pNiPAM solutions. This can be explained by the fact that TD-3 NPs are the largest, thus the same weight concentration corresponds to the largest volume fraction of the NPs. From the diffusion times τ the self-diffusion coefficient D_s can be calculated from a simple relation $\sigma^2=D_s\tau$, where σ is the Gaussian radius of the confocal volume of the microscope. The diffusion coefficient of Alexa 488 and TD-8 NPs normalized to their value at zero pNiPAM concentration (in water) are shown in Fig.18 for TD-1, TD-2, TD-3 and TD-4 solutions of different concentrations. The macroscopic viscosity is also shown there for comparison.

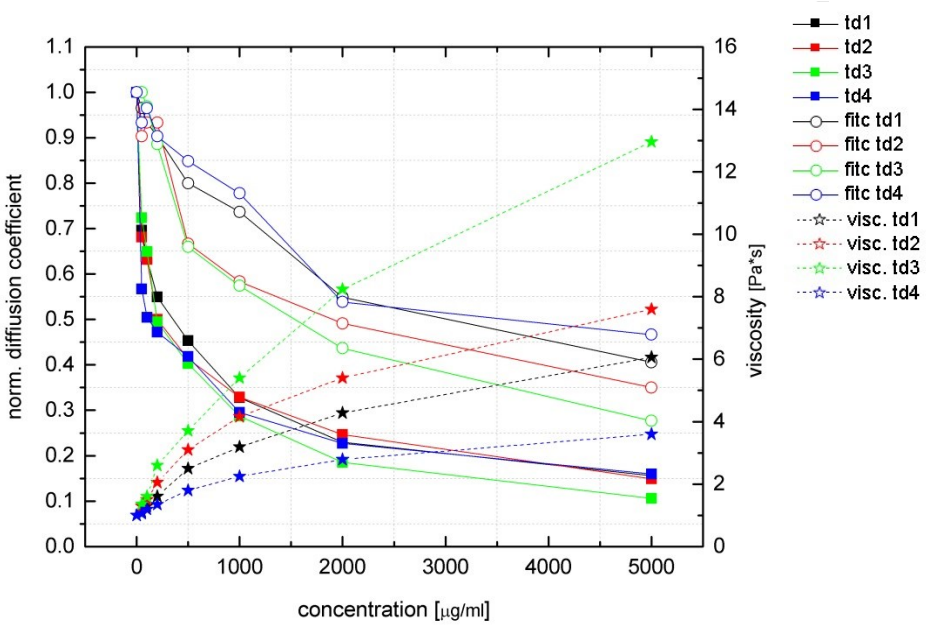

Figure 18: The normalized diffusion coefficient of Alexa488 (open symbols and solid lines) and TD-8 NPs (solid symbols and solid lines) for TD-1, TD-2, TD-3 and TD solutions of different concentrations. The macroscopic viscosity 9stars and dashed lines) is also shown for comparison.

One can clearly see in *Fig.18* that the diffusion coefficient of the TD-8 NPs decays much stronger with the increasing pNiPAM concentration than that of Alexa488. This is due to the fact that Alexa488, being small "feels" the micro viscosity. Since the size of the TD-8 NPs is large and comparable to the sizes of all other non-labeled pNiPAM NPs, it follows the macro viscosity of the solutions, as expected. In order to see better different effect of different pNiPAM samples on the diffusion of both probes, the relative change of local viscosity η/η_0 is plotted in *Fig.19.* Here η is the viscosity calculated (using the SE-relation, Eq.6) from the self-diffusion

coefficient measured with FCS and η_0 is the viscosity of solvent (at zero pNiPAM concentration) at the same temperature.

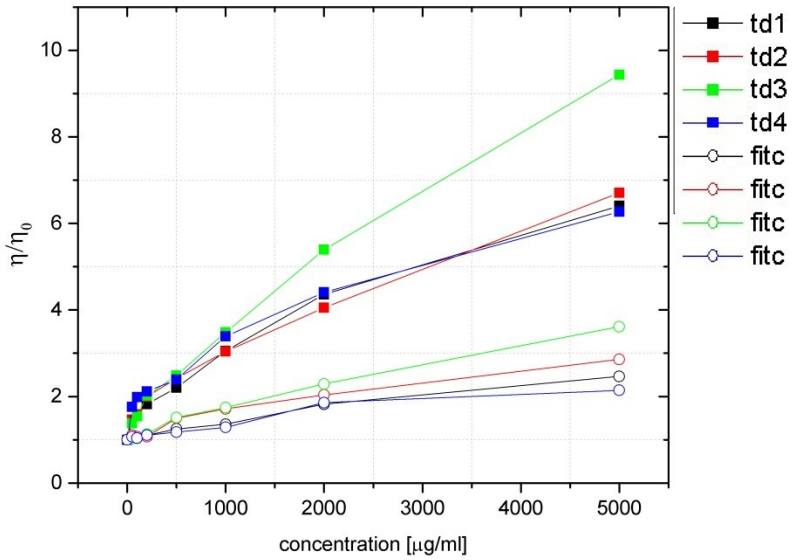

Figure 19: Normalized viscosity η/η_0 calculated (using the SE-relation, Eq. 6) from self-diffusion coefficient measured with FCS as function of pNiPAM concentration.

Figure 19 shows that the relative viscosity measured using the TD-8 NPs in all pNiPAM solutions increases much faster with increasing pNiPAM concentration than that measured with the dye. This strong effect is due to the dependence of the local viscosity of complex medium on the size of the probe. Additionally, the increase of the relative viscosity measured with both probes is the strongest in TD-3 solutions. This is due to the fact that TD-3 NPs are the largest and thus occupy the largest volume fraction of all non-labeled pNiPAM NPs.

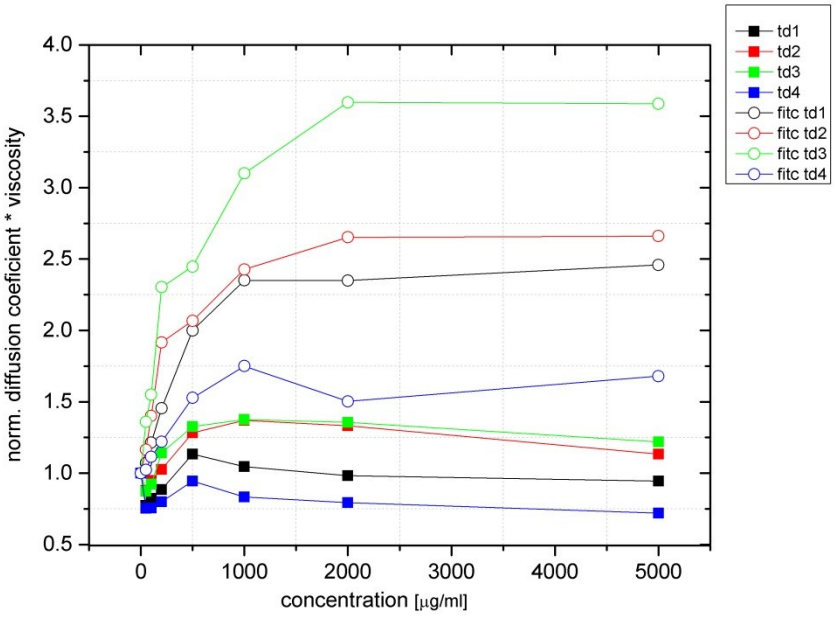

Figure 20: The product of the normalized values of the diffusion coefficient measured with FCS and macroscopic viscosity as function of pNiPAM concentration.

In Figure 20 we show the dependence of the product of the normalized diffusion coefficient of the dye and TD-8 NPs and the macroscopic viscosity on TD-1, TD-2, TD-3 and TD-4 concentration. This product is equal to the ratio of the macroscopic and microscopic viscosities, where the microscopic viscosity is that calculated from the self-diffusion coefficient using the SE relation. As one can see in Figure 20 the microscopic viscosity measured using the dye is always lower than the macroscopic viscosity while the ratio stays larger than one in almost whole range of concentration.

4.2.1.4.3. Size determination of large NPs.

A fluorescence correlation spectroscopy in a combination with a confocal microscope can also determine the hydrodynamic radius of various molecules. When fluorescently labeled nanoparticle diffuses though the confocal volume with a characteristic time which is proportional to the confocal volume, $\sigma_1^2 = D\tau$ one can determine its size based on the radius of confocal volume. This stays consistent for most particles with size not exceeding 400 nm. Any large particle or molecule with a radius comparable to the lateral confocal volume σ will remain 'visible' for a detector even outside the confocal volume and as such, requires a correction. This correction, takes into account size and shape of the particle, other diffusion modes and the distribution of the fluorescent dye within the particle. The distribution of light intensity in the focal spot during FCS experiment is approximated by a Gaussian profile using lateral and axial dimensions. What is represented as:

$$I(r) = I_0 e^{-((x^2+y^2)/2\sigma_1^2)} e^{-(z^2/(2c^2\sigma_1^2))}$$

Equation 23

Where σ_1 is the beam "radius" at $I_0/\sqrt{e}$, $c=\sigma_2/\sigma_1$ and σ_2 is the confocal volume radius in the z-direction. The value of σ_1 is equal to $\sim 0.358 r_{Airy}$ which in this case is a measure of confocal microscope optical resolution. For small fluorescent particles, for example a single dye (Alexa488), with defined D (4.3×10^{-6} cm^2/s[11]) at 20°C and σ_1 (91 nm) one can obtain τ =19.2 *μs.* In the case of large particles that

are uniformly labeled and their size is comparable or bigger than the confocal volume the normalized FCS correlation function can be calculated as:

$$G_D(t) = \int dq I_0^2(q)|B(qa)|^2 e^{-Dq^2 t}$$

Equation 24

Where:

$$|B(qa)|^2 = \left(\frac{3(\sin(qa) - qa\cos(qa))}{(qa)^3}\right)^2$$

Equation 25

$$I_0(q) = e^{-(q_x^2+q_y^2)\sigma_1^2+q_z^2c^2\sigma_1^2/2}$$

Equation 26

Now the effective beam profile can be also considered to be Gaussian.

$$I_{eff}(q) = I_0(q)|B(qa)|$$

Equation 27

The effective size of the confocal volume:

$$\sigma_{eff}^2 = \sigma_1^2 + ka^2$$

Equation 28

Since k value was reported earlier [36] [37] around k=0.22 one can conclude:

$$\frac{\tau_c}{\tau_0} = 1 + k\frac{a^2}{\sigma_1^2}$$

Equation 29

Where τ_0 is the correlation time of a particle labeled only in the center and τ_c is the fitted correlation time obtained from FCS measurements. After calculating and fitting

the correlation function with applying the form factor of uniformly labeled spheres, we obtained correlation time τ_c normalized by τ_0.

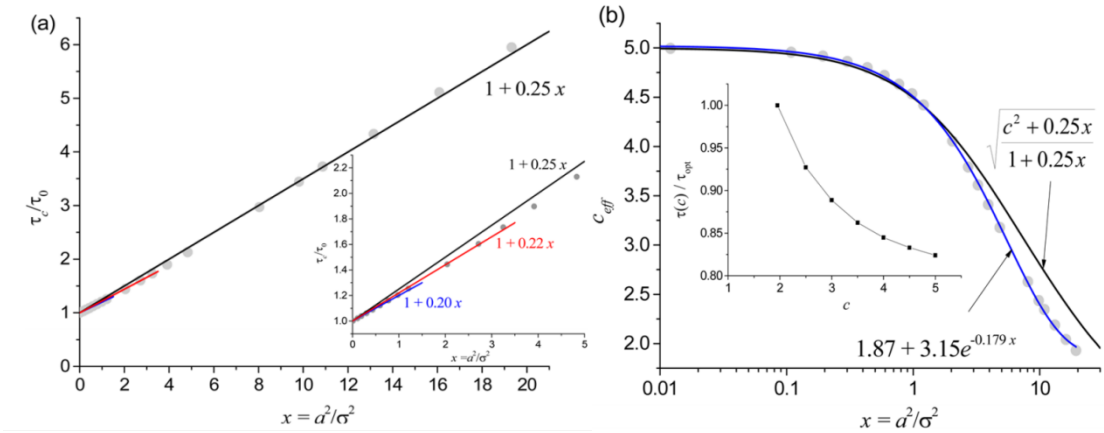

Figure 21: (a) Ratio of fitted correlation times τ_c to the corresponding values of τ_0 as a function of the squared ratio of the fluorophore radius a to the focal spot radius σ_1 defined by Equation 23. The straight lines denote the linear approximations in different ranges of $x = a^2/\sigma_1^2$. Inset: magnification of the initial part of the main plot. (b) x dependence of the c_{eff} values fitted to simulated correlation functions (points). Upper line represents the simple geometric fit to the $c_{eff}(x)$ dependence. Lower line represents a polynomial fit to the fitted $c_{eff}(x)$ dependence. The inset shows the error of the diffusion time when c is fixed in the fitting procedure to values different from the optimum one (c_{eff} = 2 in this case). [1]

One can observe that k=0.22 coefficient stays reasonable only for small values of a^2/σ_1^2 which is around 4. For smaller values, what can be seen on the Figure 21, the slope requires lower values of k (0.20). In fact maximum x values which represent the size of nanoparticle around 400nm which might be an actual size

limit for FCS experiment holds the k=0.25. Using Stockes –Einstein equation one can write:

$$(\frac{\sigma_{eff}}{\sigma_1})^2 = \frac{\tau_c/a}{\tau_r/a_r} = \frac{\sigma_1^2 + 0.25a^2}{\sigma_1^2} = 1 + 0.25\frac{a^2}{\sigma_1^2}$$

Equation 30

where a_r is the hydrodynamic radius of the reference dye. Based on this one can see that the value of k=0.25 gave the best fit in the whole range of a/σ_1(see Figure 21) and an effective correction procedure for estimating of the hydrodynamic radius for uniformly labeled spheres has been proposed [1].

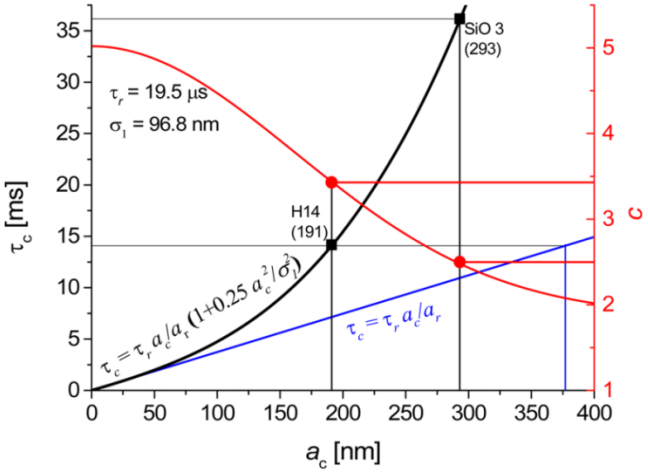

Figure 22: Procedure proposed to find the true size of the colloidal particle from a single measurement of a pair of FCS correlation times for the colloidal nanoparticle, τ_c, and the reference fluorophore, τ_r. The confocal volume size σ_1 = 96.8 nm. [1]

As it can be seen it Figure 22 to obtained the true colloidal size, a pair of FCS measurements for the colloid and the standard has to be taken. The experimental procedure is based on the following steps. First one needs to measure the diffusion time for the reference dye (τ_r), based on that calculate the $\sigma_1^2 = D\tau$ and using Equation 29

generate a plot like in Figure 22. The next step is to measure the correlation function for the sample and calculate the diffusion time of a sample (τ_c) and the *c* value from the fit. The τ_c and *c* (Figure 22) values should correspond to the same a_c. Since the fitted τ_c depends on *c* it is crucial to use the proper value of parameter *c.* That simple procedure results in the correct value of the radius for nanoparticles that are uniformly labeled and it holds in a broad range of the ratio a/σ.

4.2.2. Rheological characterization

In order to investigate rheological properties of the sample time-dependent changes should be checked. Since none was noticed (*Figure 23a*), additionally

dynamic time sweep test experiments were performed to investigate time evolution of the sample (*Figure 23b*).

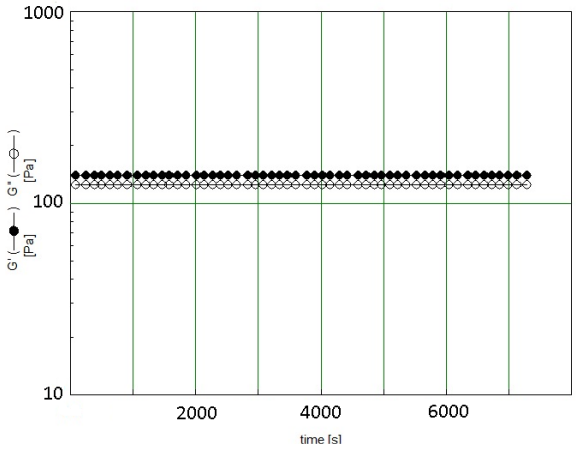

Figure 23: Time sweep test for two different time scales to investigate samples time dependency

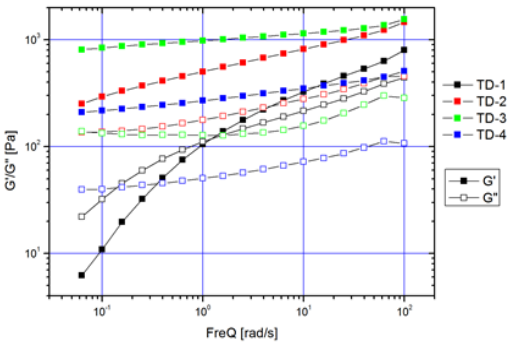

Figure 24: Dynamic Frequency Sweep for all samples at 20°C.

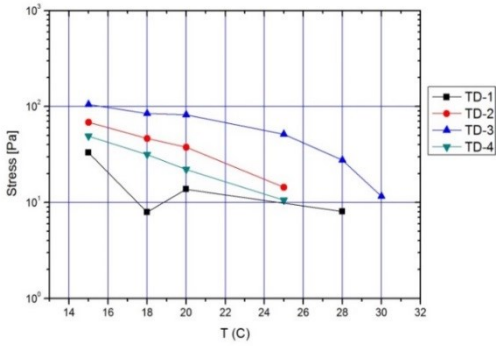

Figure 25: Yield stress as a function of temperature for all samples.

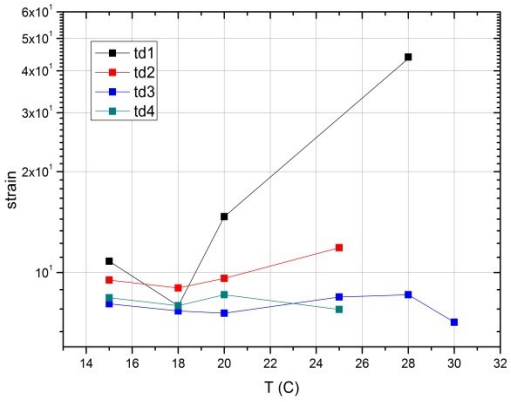

Figure 26: Yield strain as a function of temperature for all four samples.

As shown in dynamic frequency sweep test (*Fig. 24*) of four different samples three of the samples do not present a crosss-over of storage and loss moduli which represents a solid-like to liquid-like transition. With applied frequencies TD-1 is the only sample where a cross-over point below which it becomes liquid-like can be seen.

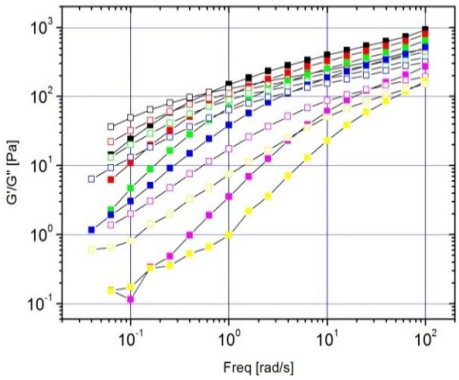

Graph 27: DFS for TD-1 at different temperatures.

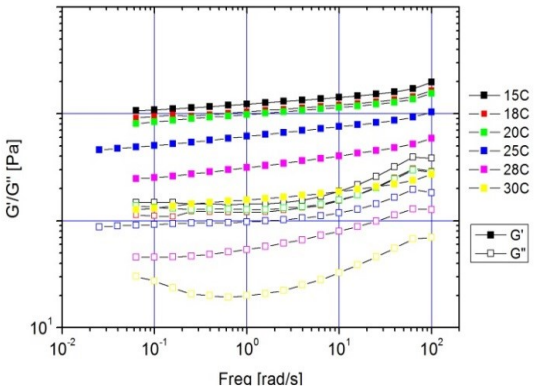

Graph 28: DFS forTD-3 at different temperatures

TD-3 and TD-4 samples as it can be seen in the Figure 24 exhibit a behavior reminiscent of colloidal glass. This seems interesting since these are the samples with the highest (*TD-3)* and the lowest (*TD-4)* volume fraction (see T*able 2*).

We believe that this difference in yielding dynamics is due to different cross-linking density which seems to be a critical factor for intrachain interactions.

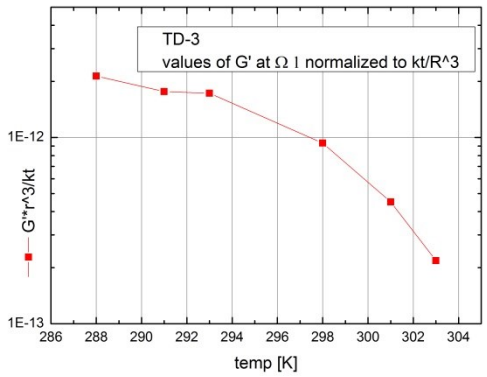

Figure 29: G' values collected at ω=1 for TD-3 sample.

Additionally TD-1 presents a drop in a stress response what is characteristic for viscoelastic systems. A proof of yielding behavior is presented in *Figures 25* and *26* for all of the samples and is due to the softening behavior what can be seen as the decrease of stress value in a range of increasing temperature [38]. From what one can observe in Figures *27 and 28 TD-1* and *TD-3* are samples which present completely different behavior in the whole range of temperatures. TD-1 in this range of temperatures relaxes faster upon increasing the temperature. This observation is consistent with a steeper decrease of the volume fraction of the pNiPAM solution when the temperature is increased.

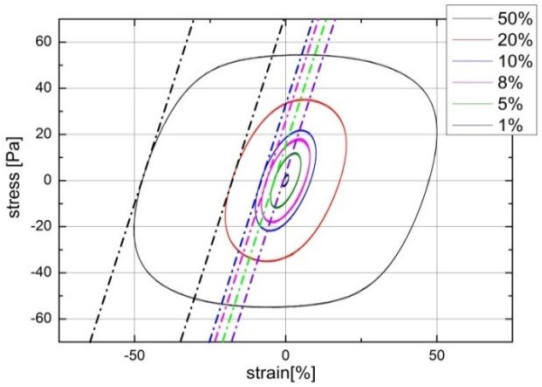

Figure 30: *Waveforms of the stress/strain response.*

	TD-3	TD-3	TD-4	TD-4
Strain [%]	G'/G" t=20C	G'/G" t=25	G'/G" t=20C	G'/G" t=25
1	378.5	235.0	145.4	71.2
5	400.5	245.5	174.4	78.2
8	462.2	304.8	150.6	82.3
10	722.5	342.5	215.4	85.3
20	482.1	276.8	281.1	99.2
50	1118.7	423.5	235.2	95.5
100	1247.3	614.9	204.7	83.8
200	1267.1	667.8	192.7	90.2
500	1275.0	590.2	251.4	96.3
1000	1130.0	561.2	195.3	75.3

Table 4: Values of cage modulus extracted from the analysis of Bowditch-Lissajou plots.

One cannot detect any crossover point for the *TD-3* sample which is solid like in whole range of temperatures investigated. What can also be seen for *TD-1* and *TD-3* samples in the lowest temperature range (15-25^{o}C) is that the change in the volume fraction is very small, consistent with R_h behavior reported in *Figure 8.* The reproducibility data (*Figures 31 and 32*) proves that there is no significant change in a system after increasing the temperature and cooling it down

to the room temperature again. To characterize the behavior of the system large amplitudes strain sweep tests were performed. The G’ and G” moduli as a function of strain amplitude at given frequency presents a typical behavior of colloidal glass with a crossover below which the system yields.

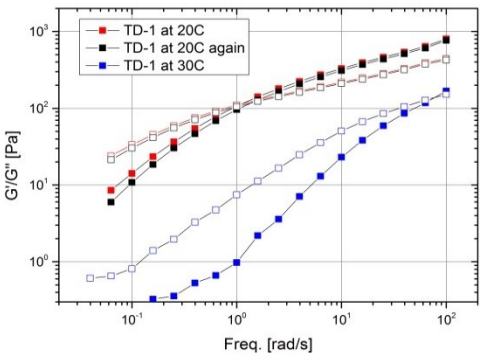

Figure 31: Dynamic frequency sweep before and after the heating

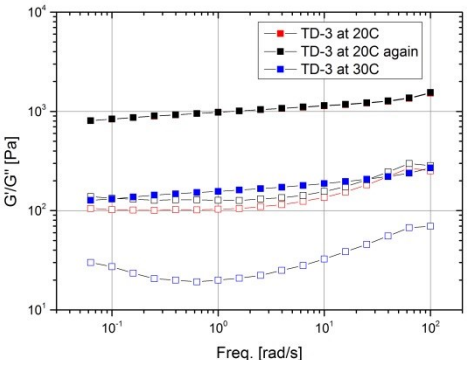

Figure 32: Dynamic strain sweep before and after the heating

A Large Amplitude Oscillatory Shear (LAOS) was employed for identifying and characterizing apparent yield stress responses in elastoviscoplastic materials [39]. Large amplitude oscillatory shear (LAOS) is a test method which systematically interconnects familiar material measures such as linear viscoelastic moduli G' and G", nonlinear viscoelastic properties allowing for nonlinear viscous and elastic effects to be characterized simultaneously. In strain-controlled LAOS deformation, the imposed strain takes the form from Equation 7. The resulting oscillatory shear stress σ is recorded and analyzed What can be seen in the behavior of the system under LAOS are the slopes at high strain amplitudes ɣ > 100%. Non-linear measurements were performed in order to extract cage modulus from the analysis of Bowditch-Lissajou plots. This Fourier Transform based analysis can

provide a better understanding of system transitions. The responses were investigated using strain-amplitude sweep tests at fixed frequency (*1 rad/s*) with strain amplitudes in the range of 1% - linear response up to 1000% to the strongly nonlinear response regime. At the Lissajou plots the similarity of the slopes at different strains can be quantify by Rogers et al[40].

$$G_{cage} = d\,stress/d\,strain|_{stress=0}$$

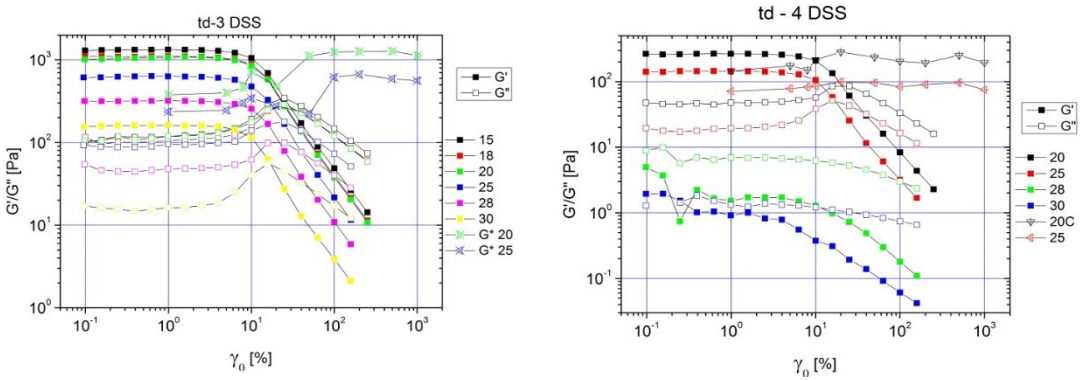

Figures 33a/b: Apparent cage modulus calculated from waveforms, plotted with dynamic strain

Apparent cage modulus in this case would be the slope value of the Lissajou figure at zero stress (*Figure 30*). Using this parameter approximately at zero global stress one can study the internal stress in the system. This so-called apparent cage modulus is a useful tool for analyzing glass-to-solid transition for glassy systems. The cage modulus calculated for each waveform is plotted with data form dynamic strain sweep test. In *Figure 33* we present completely different response from two colloidal glass systems TD-3 and TD-4. While the cage modulus rapidly increases upon yielding point for TD-3, it stays constant for TD-4. Td-3 is the most concentrated sample with highest volume fraction and the effect of imposing

large amplitude deformation represented by the increase in the apparent cage modulus can be interpreted as a result of breaking clusters/structures. The insensitivity of the apparent cage moduli at higher strains for TD-4 system would be interpreted in this case as a lack of clusters since this nanogel presents the lowest volume fraction.

4.2.2.1. Adding the linear chains

The addition of linear homopolymers can affect the static and dynamic properties of the microgels via depletion[41]. Therefore combining temperature, degree of crosslinking and depletion allows spanning a wide range of rheological response in a controlled manner.

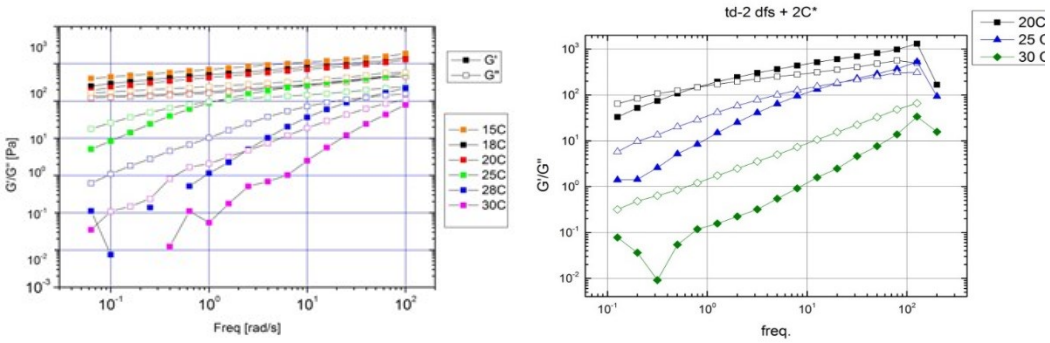

Figure 34 a/b: DFS for TD-2 in a range of temperatures and in a presence of linear chain

Here we examine transitions from solid to liquid state in the presence of linear polymer chains. Previously synthesized linear pNiPAM chains, with molecular mass M_w= 40,000 and 10,000 kg/mol were employed. Linear polymer chains were added to pNiPAM nanogel solutions at different concentrations: for 10,000 M_w linear pNiPAM in a range 0,5 to 6 C* (overlapping concentrations) and for 40,000

M_w linear pNiPAM 1C* and 2C*. Linear and non-linear rheology measurements for the mixture were performed. In the absence of linear chains, all the pNiPAM solution, except TD-1 exhibit glassy behavior with both, G' and G" modulus weakly frequency-dependent. What can be seen in *Figure 34a* and *34b*, increased frequency-dependence of a G' moduli for TD-2 upon adding the linear chains (40,000 M_w) including new cross-over at 20°C and a shift of liquid transition towards higher frequencies.

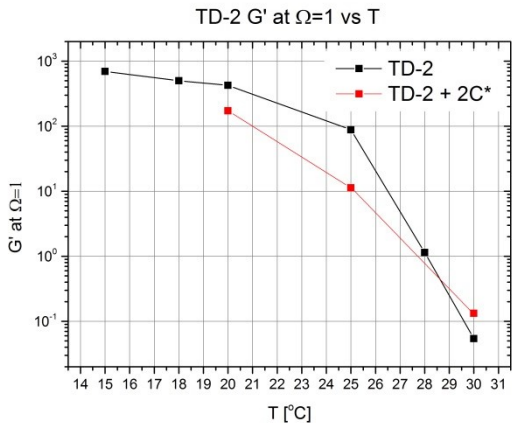

Figure 35: Values of G' at ω=1 as a function of temperature.

A general decrease for both G'/G" moduli should be considered as softening of the system. By adding the big linear chains we can observe a depletion mechanism based on creating an osmotic force that shrinks the particles. This phenomenon is consistent with the previous founding for hard spheres and star polymers [42]. It is interesting to note that the sample with higher volume fraction - TD-3, becomes more solid-like upon adding the linear chains both for 10,000 and 40,000 M_w. Upon adding 1C* and 2C* of the linear chains one can observe a gradual increase of G'/G" moduli (*see Figure 36b and 36c*). This suggests a possible penetration of

the linear chains into the particles and is consistent with the DLS data confirming that the particles R_h increasing upon adding the linear chains (Figure *36d*). Additionally, calculated mesh size (see *table 2*; for TD-3 is more than two times bigger) explains the different changes in hydrodynamic radius measured by DLS upon adding the linear chain for a both polymers.

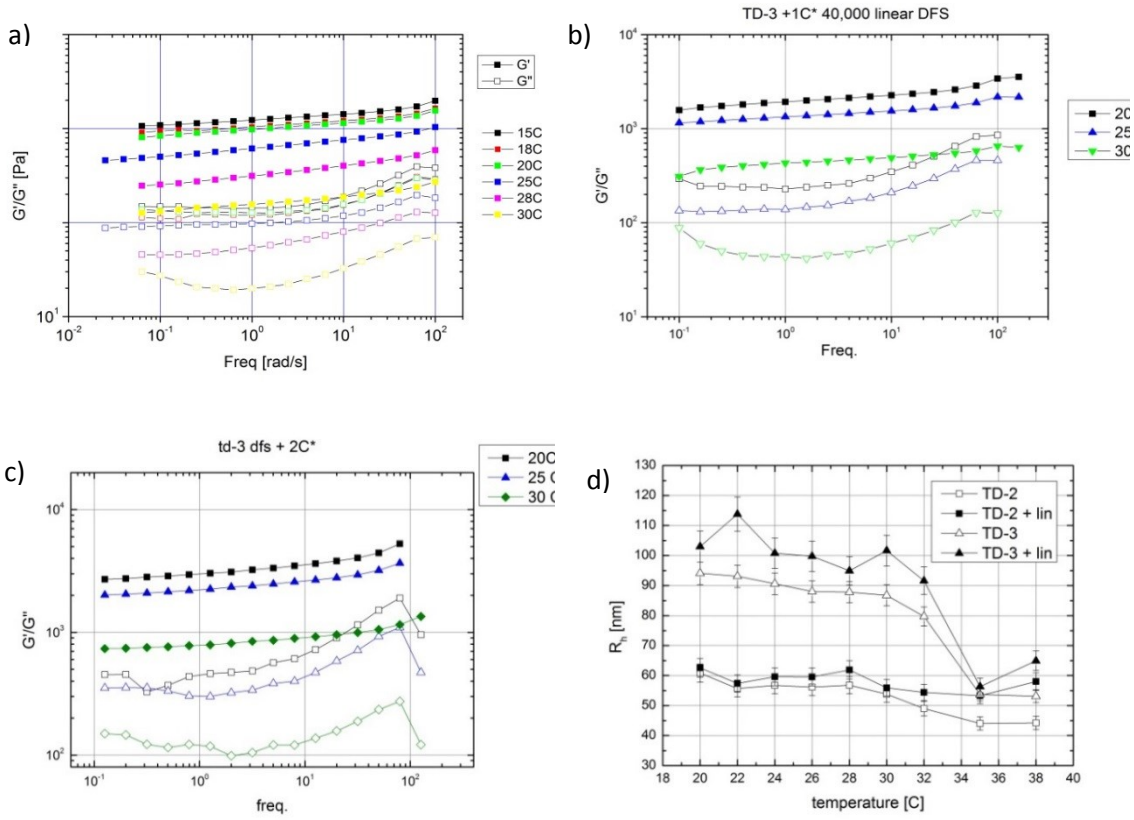

e)

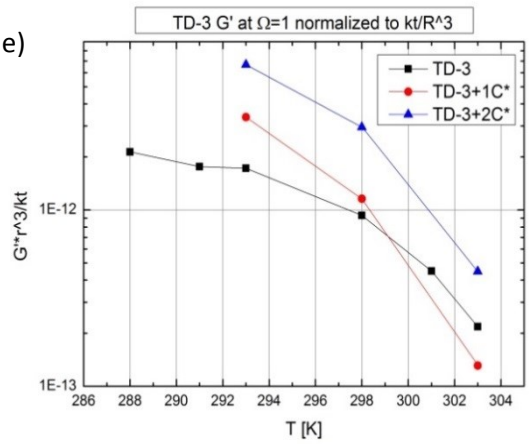

Figure 36:
a) Dynamic Frequency Sweep forTD-3 at different temperatures
b) Dynamic Frequency Sweep forTD-3 with 1C* of linear chain
c) Dynamic Frequency Sweep forTD-3 with 2C* of linear chain
d) DLS data for TD-2 and TD-3 samples with/without linear chain (40,000 Mw)
e) TD-3 upon adding linear chain at Ω=1

4.3. Biocompatibility

Regarding the potential applications of the pNiPAM nanoparticles a vast majority of it will require introducing the particles into the biological system. The biocompatibility and toxicity of pNiPAM nanoparticles is clearly a crucial issue. The cytotoxicity of thermo-responsive pNiPAM nanoparticles was studied followed by a detailed analysis of NPs morphology in growing cell cultures and their 3D structure.

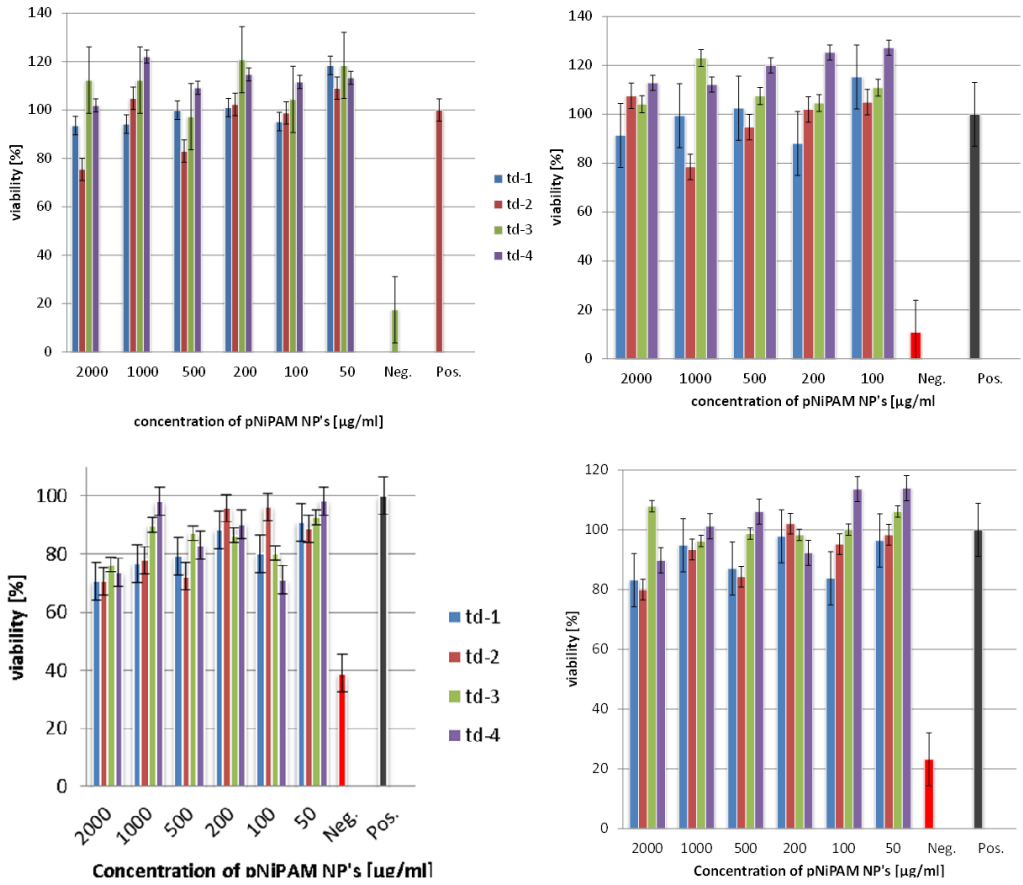

Figure 37: Percentage of metabolic active cell as the result from MTT assay for HeLa and HEK293 cell lines examined after 24 and 48 hours respectively.

Cytotoxicity examination was conducted for two cell cultures - HeLa (cervical cancer cell line) and HeK293 (human embryonic kidney cell line) cell employing MTT (3-4, 5-dimethylthiazol-2-yl-2,5-diphenyltetrazolium bromide) assay and viability tests.

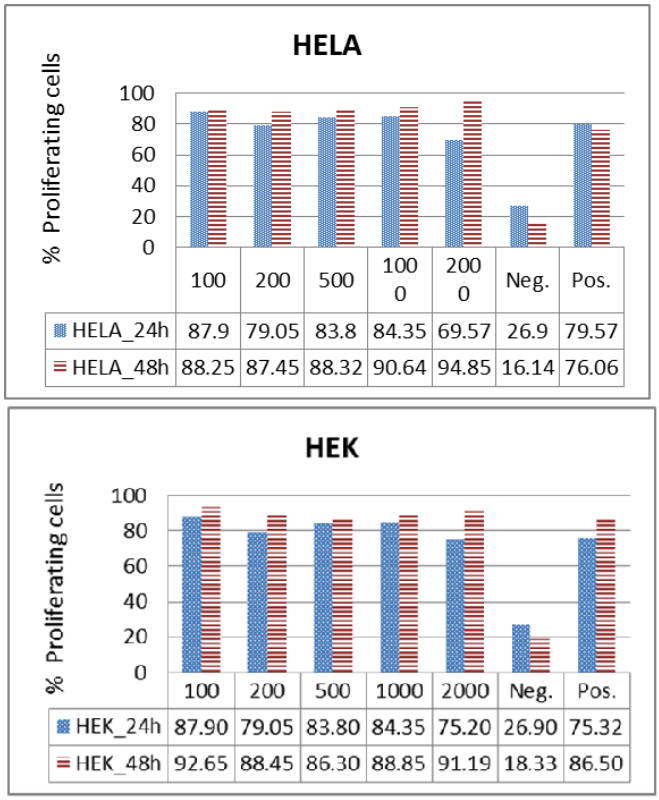

Figure 38: Percentage of proliferating HeLa and HEK293 cells, versus added concentration of TD-# NPs [µg/ml]. Neg is negative probe with DMSO added and Pos is control one with no additional factors.

Potential cytotoxic effects are crucial for any bio-material and require more detailed tests, that can determine: (i) biocompatibility of pNiPAM nanoparticles, (ii) cell line viability and proliferation capabilities after introducing nanoparticles and (iii) cell capability for growth directly on the pNiPAM NPs surface [43], [44]. Using the MTT assay considered to be a standard cytotoxicity test we can report no cytotoxicity effects in the tested cell lines at the concentration used for several different pNiPAM nanoparticles (*Figure 37*), in agreement with previous reports [45]. As it can be seen in F*igures 37* all of the examined pNiPAM concentrations did not affect cell lines substantially. One can also notice that in the presence of

pNiPAM NPs, cellular metabolic activity is clearly higher than in probe without the NPs (*Pos.* - positive) for both HeLa and for HEK293 cell cultures seeded for 48 h. What needs to be pointed out is that considering the reference (*Pos*. - positive) probe as fully supplied in terms of nutrition, samples exhibiting more than 100% of the reference activity should be considered as containing an additional viability promoting factor. To investigate this phenomenon and to double check these data, a proliferation test was performed. A higher proliferation activity of cells was observed upon addition of pNiPAM polymer in comparison to the positive control, for majority of nanoparticle concentrations used (*Figure 38)* what is consistent with data obtained from metabolic activity tests. As the cells proliferates the diffusion of nutritious is more and more difficult within this artificial environment thus the presence of pNiPAM NPs can be an essential factor for longer cell culture growth. As expected, the most significant increase in proliferation percentage was observed for lower concentrations of NPs. Above all no significant decrease in cell viability for any of the pNiPAM systems in the range of the examined concentrations was observed which can be interpreted as a lack of cytotoxicity. For the TD-3 sample (the sample with the largest NPs size, see T*able. 2*) the result clearly shows that there is no decrease in cell proliferation capability in the presence of pNiPAM nanoparticles (*Figure 38*).

4.3.1. pNiPAM as a potential bio-scaffold

Based on previous studies [27] and considering our experimental results - lack of cytotoxicity and additionally an increase of viability due to the pNiPAM NPs presence, suggest that pNiPAM is forming the so-called bio-scaffold which is promoting cell growth and might be used for cell cultivation. To confirm this hypothesis, Cryo-SEM were performed and pictures of pNiPAM NPs networks were analyzed. This morphological evaluation of the pNiPAM layer on glass was performed using Cryo-SEM and it is shown in *Fig.* 39, with increasing magnification. It can be clearly seen in these figures that pNiPAM nanoparticles used at high concentrations form a network of 3D scaffold which includes porous layers with buffer trapped inside. These images give clear information how the scaffold is formed in cell culture plates. Clusters of nanoparticles support the growth of cells by aggregating into a sub-micron porous structure which is deposited on surface of the cell plate. The fact that the scaffolds can be formed creates a way for efficient distribution of the nutrients within its pores. Due to the presence of polymeric network a better dispersal of the nutrients is being observed and as a result an increase in proliferation and cell viability had been noticed.

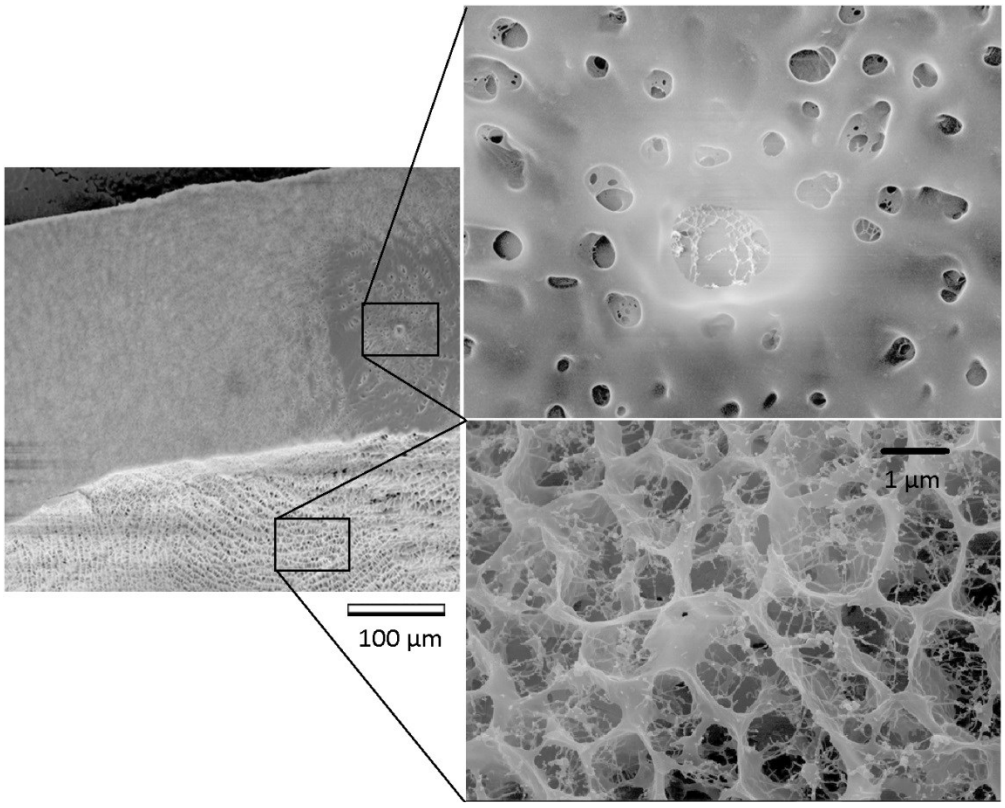

Figure 37: CRYO- SEM pictures of pNiPAM microgel; showing the surface and the interior of a polymer network.

5. CONCLUSIONS

Well defined poly-N-isopropylacrylamide (pNiPAM) nanoparticles with various sizes, volume fraction, mesh size and the cross-linking degree were synthesized. As a result of emulsion free radical polymerization the swelling ratio of the pNiPAM nanoparticles increases with decreasing SDS and crosslinker concentration quite consistently.

Obtained nanoparticles have been proven to be stimuli responsive as they undergo a reversible phase transition above 33^{o}C. This phenomenon called LCST occurs around natural human body temperature thus, it is a good model for a drug delivery system.

All of the synthesized nanoparticles form a microgel thus the rheological characterization took place. Synthesized pNiPAM microgel NPs presented basically two different behaviors typical for colloids and colloidal glass.

PNiPAM nanoparticles were then functionalized with fluorescent dye applying two different approaches for incorporating the dye into to the polymer network. FCS investigation shows that incorporating fluorescent dye into the polymer network as a cross-linker is less efficient for fluorescence based studies than using the co-monomeric labeled pNiPAM. Functionalized pNiPAM NP's with a fluorescent dye as a co-monomer represent a stable fluorescence meaning that the samples did not change significantly in terms of diffusion times and fluorescence intensity for the same dilution in over two years of measurements, thus, they can be used for investigations employing various fluorescent techniques.

The internal packing of the NPs and their behavior in solutions at different concentrations was studied by comparing the micro-viscosity measured by FCS to the macro-viscosity obtained from viscometer.

The correction method was proposed for the correct size determination by FCS for large NPs of sizes comparable to the radius of the confocal volume.

What is important in developing any system with potential bio-application is its toxicity. The cytotoxicity tests of the thermo-responsive pNiPAM hydrogel nanoparticles have clearly demonstrated the lack of their cytotoxicity for the HeLa and HEK293 cell lines. Additionally in the presence of pNiPAm NPs, cells tend to exhibits higher metabolic activity and proliferation. More detail test investigating the nanoscale structure of the polymer network and in-vivo imaging proved that pNiPAM is forming a bio scaffold that positively effects cells growth.

RERERENCES

1. Deptuła, T.; Buitenhuis, J.; Jarzębski, M.; Patkowski, A.; Gapinski, J., Size of Submicrometer Particles Measured by FCS: Correction of the Confocal Volume. *Langmuir : the ACS journal of surfaces and colloids* **2015,** *31* (24), 6681-6687.
2. Dogu, Y.; Okay, O., Swelling–deswelling kinetics of poly(N-isopropylacrylamide) hydrogels formed in PEG solutions. *Journal of Applied Polymer Science* **2006,** *99* (1), 37-44.
3. Fu, J.; Chen, L.; Li, J.; Zhang, Z., Current status and challenges of ion imprinting. *Journal of Materials Chemistry A* **2015,** *3* (26), 13598-13627.
4. Lee, W.-F.; Lu, H.-C., Synthesis and swelling behavior of thermosensitive IPN hydrogels based on sodium acrylate and N-isopropyl acrylamide by a two-step method. *Journal of Applied Polymer Science* **2013,** *127* (5), 3663-3672.
5. Kadajji, V. G.; Betageri, G. V., Water Soluble Polymers for Pharmaceutical Applications. *Polymers* **2011,** *3* (4), 1972.
6. (a) Li, L. Y.; He, W. D.; Li, J.; Zhang, B. Y.; Pan, T. T.; Sun, X. L.; Ding, Z. L., Shell-cross-linked micelles from PNIPAM-b-(PLL)2 Y-shaped miktoarm star copolymer as drug carriers. *Biomacromolecules* **2010,** *11* (7), 1882-90; (b) Huang, G.; Gao, J.; Hu, Z.; St John, J. V.; Ponder, B. C.; Moro, D., Controlled drug release from hydrogel nanoparticle networks. *Journal of controlled release : official journal of the Controlled Release Society* **2004,** *94* (2-3), 303-11.
7. Rashmi R Kokardekar, V. K. S. a. H. R. M., PNIPAM Poly (N-isopropylacrylamide): A Thermoresponsive “Smart”

Polymer in Novel Drug Delivery Systems *Internet Journal of Medical Update* **2011**.
8. Fan, L.; Wu, H.; Zhang, H.; Li, F.; Yang, T.-h., pH-sensitive Podophyllotoxin carrier for cancer cells specific delivery. *Polymer Composites* **2010,** *31* (1), 51-59.
9. Ravichandran, R., Nanotechnology Based Drug Delivery System. *NanoBiotechnnology* **2009,** *5* (1-4), 17-33.
10. Brigger, I.; Dubernet, C.; Couvreur, P., Nanoparticles in cancer therapy and diagnosis. *Advanced drug delivery reviews* **2002,** *54* (5), 631-51.
11. Zhang, G.; Yang, N.; Ni, Y.; Shen, J.; Zhao, W.; Huang, X., A H2O2 electrochemical biosensor based on biocompatible PNIPAM-g-P (NIPAM-co-St) nanoparticles and multi-walled carbon nanotubes modified glass carbon electrode. *Sensors and Actuators B: Chemical* **2011,** *158* (1), 130-137.
12. Parasuraman, D.; Sarker, A. K.; Serpe, M. J., Poly(N-isopropylacrylamide)-based microgels and their assemblies for organic-molecule removal from water. *Chemphyschem : a European journal of chemical physics and physical chemistry* **2012,** *13* (10), 2507-15.
13. Li, G.; Song, S.; Zhang, T.; Qi, M.; Liu, J., pH-sensitive polyelectrolyte complex micelles assembled from CS-g-PNIPAM and ALG-g-P(NIPAM-co-NVP) for drug delivery. *International journal of biological macromolecules* **2013,** *62*, 203-10.
14. Karg, M.; Pastoriza-Santos, I.; Rodriguez-Gonzalez, B.; von Klitzing, R.; Wellert, S.; Hellweg, T., Temperature, pH, and ionic strength induced changes of the swelling behavior of PNIPAM-poly(allylacetic acid) copolymer microgels. *Langmuir : the ACS journal of surfaces and colloids* **2008,** *24* (12), 6300-6.
15. Gao, X.; Cao, Y.; Song, X.; Zhang, Z.; Xiao, C.; He, C.; Chen, X., pH- and thermo-responsive poly(N-isopropylacrylamide-co-acrylic acid derivative) copolymers and

hydrogels with LCST dependent on pH and alkyl side groups. *Journal of Materials Chemistry B* **2013,** *1* (41), 5578-5587.
16. Sharma, A. K.; Sharma, Y.; Duhan, S., Biocompatible Smart Matrices Based on Poly (3,4-ethylenedioxythiophene)-Poly (N-isopropylacrylamide) Composite. *International Journal of Polymeric Materials and Polymeric Biomaterials* **2014,** *64* (7), 333-337.
17. Halima, A.; Aleksandra, S.; Thibault, R.-C.; Jaafar, G.; Raphaël, S., Thermo-responsive and aqueous dispersible ZnO/PNIPAM core/shell nanoparticles. *Nanotechnology* **2015,** *26* (33), 335605.
18. Liu, Y.-Y.; Lan, S.; Xiao, L.-Q., Synthesis and Characterization of PNIPAm Core Cross-Linked Star Polymers and Their Functionalization with Cyclodextrin. *Macromolecular Chemistry and Physics* **2015,** *216* (7), 749-760.
19. Tieqiang, W.; Shuli, W.; Xun, Z.; Guoshuai, S.; Ye, Y.; Xinyang, C.; Yu, F.; Junhu, Z.; Bai, Y., Responsive etalon based on PNIPAM@SiO 2 composite spacer with rapid response rate and excellent repeatability for sensing application. *Nanotechnology* **2015,** *26* (28), 285501.
20. Bergueiro, J.; Calderón, M., Thermoresponsive Nanodevices in Biomedical Applications. *Macromolecular Bioscience* **2015,** *15* (2), 183-199.
21. Han, D.-M.; Matthew Zhang, Q.; Serpe, M. J., Poly (N-isopropylacrylamide)-co-(acrylic acid) microgel/Ag nanoparticle hybrids for the colorimetric sensing of H2O2. *Nanoscale* **2015,** *7* (6), 2784-2789.
22. Shibayama, M.; Tanaka, T., VOLUME PHASE-TRANSITION AND RELATED PHENOMENA OF POLYMER GELS. *Advances in Polymer Science* **1993,** *109*, 1-62.
23. Hoffman, A. S., "Intelligent" polymers in medicine and biotechnology. *Artificial organs* **1995,** *19* (5), 458-67.
24. Duncan, R., The dawning era of polymer therapeutics. *Nat Rev Drug Discov* **2003,** *2* (5), 347-360.
25. Ma, Y.; Liu, S.; Yang, H.; Wu, Y.; Sun, H.; Wang, J.; Zhao, Q.; Li, F.; Huang, W., A water-soluble phosphorescent polymer for time-resolved assay and bioimaging of cysteine/homocysteine. *Journal of Materials Chemistry B* **2013,** *1* (3), 319-329.
26. Cooperstein, M. A.; Canavan, H. E., Biological cell detachment from poly(N-isopropyl acrylamide) and its applications. *Langmuir : the ACS journal of surfaces and colloids* **2010,** *26* (11), 7695-707.
27. Cooperstein, M. A.; Canavan, H. E., Assessment of cytotoxicity of (N-isopropyl acrylamide) and Poly(N-isopropyl acrylamide)-coated surfaces. *Biointerphases* **2013,** *8* (1), 23.
28. Maheswari, B.; Babu, P. E.; Agarwal, M., Role of N-vinyl-2-pyrrolidinone on the thermoresponsive behavior of PNIPAm hydrogel and its release kinetics using dye and vitamin-B12 as model drug. *Journal of biomaterials science. Polymer edition* **2014,** *25* (3), 269-86.
29. John, T., *Philosophical Magazine* **1869,** *37, 1869,* (384; 38, 1869, 156.).
30. Rayleigh, L., *Philosophical Magazine* **1871,** *41, 1871,* (107, 274, 447.).
31. Christopoulou, C.; Petekidis, G.; Erwin, B.; Cloitre, M.; Vlassopoulos, D., Ageing and yield behaviour in model soft colloidal glasses. *Philosophical transactions. Series A, Mathematical, physical, and engineering sciences* **2009,** *367* (1909), 5051-71.
32. Still, T.; Chen, K.; Alsayed, A. M.; Aptowicz, K. B.; Yodh, A. G., Synthesis of micrometer-size poly(N-isopropylacrylamide) microgel particles with homogeneous

crosslinker density and diameter control. *Journal of Colloid and Interface Science* **2013,** *405*, 96-102.
33. Fanger, C.; Wack, H.; Ulbricht, M., Macroporous Poly(N-isopropylacrylamide) hydrogels with adjustable size "cut-off" for the efficient and reversible immobilization of biomacromolecules. *Macromol Biosci* **2006,** *6* (6), 393-402.
34. Canal, T.; Peppas, N. A., Correlation between mesh size and equilibrium degree of swelling of polymeric networks. *Journal of biomedical materials research* **1989,** *23* (10), 1183-93.
35. Szymanski, J.; Patkowski, A.; Wilk, A.; Garstecki, P.; Holyst, R., Diffusion and viscosity in a crowded environment: from nano- to macroscale. *The journal of physical chemistry. B* **2006,** *110* (51), 25593-7.
36. Kang, K.; Gapinski, J.; Lettinga, M. P.; Buitenhuis, J.; Meier, G.; Ratajczyk, M.; Dhont, J. K. G.; Patkowski, A., Diffusion of spheres in crowded suspensions of rods. *The Journal of Chemical Physics* **2005,** *122* (4), 044905.
37. Price, W. S.; Price, W. S., *Diffusion and its measurement*

NMR Studies of Translational Motion. Cambridge University Press: 2009.
38. Truzzolillo, D.; Vlassopoulos, D.; Gauthier, M., Rheological detection of caging and solid–liquid transitions in soft colloid–polymer mixtures. *Journal of Non-Newtonian Fluid Mechanics* **2013,** *193* (0), 11-20.
39. Ewoldt, R.; Winter, P.; Maxey, J.; McKinley, G., Large amplitude oscillatory shear of pseudoplastic and elastoviscoplastic materials. *Rheol Acta* **2010,** *49* (2), 191-212.
40. Rogers, S. A.; Erwin, B. M.; Vlassopoulos, D.; Cloitre, M., A sequence of physical processes determined and quantified in LAOS: Application to a yield stress fluid. *Journal of Rheology (1978-present)* **2011,** *55* (2), 435-458.
41. Stiakakis, E.; Petekidis, G.; Vlassopoulos, D.; Likos, C. N.; Iatrou, H.; Hadjichristidis, N.; Roovers, J., Depletion and cluster formation in soft colloid - polymer mixtures. *EPL (Europhysics Letters)* **2005,** *72* (4), 664.
42. D. Vlassopoulos, E. S., M. Kapnistos, *Rheology Reviews* **2007**, 179 - 252.
43. Vihola, H.; Laukkanen, A.; Valtola, L.; Tenhu, H.; Hirvonen, J., Cytotoxicity of thermosensitive polymers poly(N-isopropylacrylamide), poly(N-vinylcaprolactam) and amphiphilically modified poly(N-vinylcaprolactam). *Biomaterials* **2005,** *26* (16), 3055-3064.
44. Hussien, R.; Rihn, B. H.; Eidi, H.; Ronzani, C.; Joubert, O.; Ferrari, L.; Vazquez, O.; Kaufer, D.; Brooks, G. A., Unique growth pattern of human mammary epithelial cells induced by polymeric nanoparticles. *Physiological reports* **2013,** *1* (4), e00027.
45. Wadajkar, A.; Koppolu, B.; Rahimi, M.; Nguyen, K., Cytotoxic evaluation of N-isopropylacrylamide monomers and temperature-sensitive poly(N-isopropylacrylamide) nanoparticles. *J Nanopart Res* **2009,** *11* (6), 1375-1382.